

**DEVELOPMENT OF FUNCTIONALLY GRADED DENTAL
POST BASED ON A NOVEL SILICA-COATED TITANIUM
POWDER AND HYDROXYAPATITE**

BY

NUR FARHA BINTI ABDUL HALIM

**DISSERTATION SUBMITTED IN FULFILLMENT OF THE
REQUIREMENTS FOR THE DEGREE OF MASTER OF
DENTAL SCIENCE**

**FACULTY OF DENTISTRY
UNIVERSITY OF MALAYA
KUALA LUMPUR**

2017

ABSTRACT

Introduction: Biomedical-graded metallic compounds such as titanium, stainless steel, and their alloys are potential components for fabrication of load-bearing implants due to their favorable mechanical behavior. The facile chemical and surface modification of these compounds also allows alteration of various biological and physical properties according to their intended application.

Purposes: The purpose of this study was to investigate the effect of surface modification of titanium (Ti) particles by a silica protective layer on the physical, chemical and mechanical properties of hydroxyapatite-titanium (HA-Ti) composites. The new type of fabrication and characterization functionally graded material (FGM) using hydroxyapatite (HA) and silica-coated titanium (STP) were also applied in this study.

Methods: It is well known that the formation of phases such as Ti_xP_y and $CaTiO_3$ at elevated temperatures results in a fragile behaviour of the material without displaying any yield stress prior to the rupture, providing a weak interface bonding in the matrix. As particular approaches to remove the fragile compounds, utilization of STP particles and incorporation of low-melting-point biocompatible additives as a sintering aid. In the first phase, Ti particles were coated by thin silica layers prior to mixing with HA to prevent the undesired reactions between HA and Ti. In the second phase, developed FGM composites were successfully applied for development of thermo-mechanically stable FGMs, suitable for fabrication of load-bearing heterogeneous implants such as dental posts.

Results: The decomposition of HA and oxidation of the Ti during the sintering process occurred at $1100^{\circ}C$. However, the undesired interaction between HA and Ti components were minimized, causing the complete removal of calcium titanate, $CaTiO_3$ and titanate phosphides, Ti_xP_y as well as the formation of stable calcium phosphate, CaP in the

sintered composite. In the addition of silica, SiO_2 resulted in the formation of calcium silicates (mostly CaSiO_3), which this compound may exhibit less negative impact on the mechanical properties compared to CaTiO_3 and Ti_xP_y . According to the Vickers' hardness value, composites containing identical weight ratios of HA and STP exhibited a relatively high value comparable to that of HA-Ti composites with a weight ratio of 3:1.

Conclusion: Surface modification of titanium particles using a silica layer could significantly improve the mechanical properties of the obtained composites by increasing their thermal stability during the sintering process. As a novel of metallic-ceramic FGMs, it allows one-step facile fabrication of functionally graded dental posts (FGDPs) without the necessity of performing costly and time consuming sintering process.

ABSTRAK

Pengenalan: Kompaun logam bergred biomedikal seperti titanium, keluli nirkarat, dan aloi adalah komponen yang berpotensi untuk fabrikasi implan gelas beban kerana penggalak tindakan mekanikalnya. Kelancaran kimia dan permukaan pengubahsuaian sebatian ini juga membolehkan perubahan pelbagai sifat-sifat biologi dan fizikal mengikut aplikasi yang diperlukan.

Tujuan: Kajian ini bertujuan mengkaji kesan pengubahsuaian permukaan zarah titanium (Ti) oleh lapisan pelindung silika pada fizikal, kimia dan sifat mekanik komposit hydroxyapatite-titanium (HA-Ti). Jenis baru fabrikasi dan pencirian bahan berfungsi bergred (FGM) menggunakan hydroxyapatite (HA) dan silika bersalut titanium (STP) juga digunakan dalam kajian ini.

Kaedah: Adalah diketahui umum bahawa pembentukan fasa seperti Ti_xP_y dan $CaTiO_3$ pada suhu tinggi memberikan keputusan dalam keadaan bahan rapuh tanpa memaparkan sebarang tegasan alah sebelum pecah, termasuk menyediakan ikatan antara muka yang lemah dalam matriks. Sebagai pendekatan tertentu untuk menyingkirkan sebatian rapuh, penggunaan partikel STP dan penggabungan takat lebur rendah bahan tambahan bioserasi sebagai bantuan pensinteran. Dalam fasa pertama, zarah Ti telah disalut oleh lapisan silika nipis sebelum dicampurkan dengan HA untuk mengelakkan tindak balas yang tidak diingini antara HA dan Ti. Dalam fasa kedua, komposit FGM yang berkembang telah berjaya digunakan untuk pembangunan FGMs yang termo-mekanikalnya stabil, sesuai untuk fabrikasi implan heterogen gelas beban seperti tiang gigi.

Keputusan: Penguraian HA dan pengoksidaan Ti telah berlaku semasa proses pembakaran berlaku pada 1100°C . Walau bagaimanapun, interaksi yang tidak diingini antara HA dan komponen Ti telah dikurangkan, menyebabkan penyingkiran yang

lengkap kalsium titanat, CaTiO_3 dan titanat phosphides, Ti_xP_y serta pembentukan kalsium fosfat yang stabil, CaP dalam komposit pensinteran. Dalam penambahan silika, SiO_2 mengakibatkan pembentukan silikat kalsium (kebanyakannya CaSiO_3), yang sebatian ini mungkin menunjukkan kurang kesan negatif ke atas sifat-sifat mekanikal berbanding CaTiO_3 dan Ti_xP_y . Menurut nilai kekerasan Vickers', komposit yang mengandungi nisbah berat serupa antara HA dan STP menunjukkan nilai relatif yang tinggi berbanding dengan komposit HA-Ti dengan nisbah berat 3:1.

Kesimpulan: Pengubahsuaian permukaan zarah titanium menggunakan lapisan silika boleh meningkatkan sifat-sifat mekanikal bagi komposit yang diperoleh dengan meningkatkan kestabilan terma semasa proses pensinteran. Sebagai novel FGMs logam-seramik, fabrikasi satu-langkah fungsi digred tiang pergigian (FGDPs) tanpa perlu melaksanakan proses pensinteran yang mahal dan memakan masa.

UNIVERSITY OF MALAYA

ORIGINAL LITERARY WORK DECLARATION

Name of Candidate: Nur Farha Binti Abdul Halim (I.C No: 881009-07-5184)

Registration/Matric No: DGC 140002

Name of Degree: Master of Dental Science in Restorative Dentistry

Title of Research Report: **Development of Functionally Graded Dental Post Based on a Novel Silica-Coated Titanium Powder and Hydroxyapatite**

Field of Study: Restorative Dentistry

I do solemnly and sincerely declare that:

- (1) I am the sole author/writer of this work;
- (2) This work is original;
- (3) Any use of any work in which copyright exists was done by way of fair dealing and for permitted purposes and any excerpt or extract from, or reference to or reproduction of any copyright work has been disclosed expressly and sufficiently and the title of the Work and its authorship have been acknowledged in this work;
- (4) I do not have any actual knowledge nor do I ought reasonably to know that the making of this work constitutes an infringement of any copyright work;
- (5) I hereby assign all and every rights in the copyright to this work to the University of Malaya ("UM"), who henceforth shall be owner of the copyright in this work and that any reproduction or use in any form or by any means whatsoever is prohibited without the written consent of UM having been first had and obtained;
- (6) I am fully aware that if in the course of making this work I have infringed any copyright whether intentionally or otherwise, I may be subject to legal action or any other action as may be determined by UM.

Candidate's Signature

Date:

Subscribed and solemnly declared before,

Witness's Signature

Date:

Name: Dr. Hadijah Binti Abdullah

Designation: Associate Professor, Department of Restorative Dentistry, Faculty of Dentistry, University of Malaya, Kuala Lumpur, Malaysia.

ACKNOWLEDGEMENTS

All praises and glory to Almighty Allah S.W.T for bestowing countless blessings, including physical robustness in me, on account of which I was able to complete this thesis. I humbly offer salutations upon Prophet of Muhammad S.A.W, the source of guidance and knowledge to all mankind.

I am grateful and highly indebted to my research advisors, Prof. Madya Dr. Hadijah Abdullah (Associate Professor, Restorative Department, Faculty of Dentistry) and Dr. Muralithran Govindan Kutty (Material Science Lecturer, Restorative Department, Faculty of Dentistry). I extend my heartfelt respect for their unflagging encouragement and diligent supervisions. Their co-operative and amiable nature is indeed exemplary. In point of fact, I was doubly blessed as I also worked under guidance of Dr. Ali Dabbagh (Post Doc, IPPP UM). His useful comments and counseling has led to significant achievements in this work.

I would also like to extend my sincerest gratitude to Prof. Dr. Noor Hayaty Abu Kasim and Prof. Madya Dr. Noor Lide Abu Kassim for their great pleasure to interact, supporting and encouraging me to go on and never give up if I faced any difficulties in my life. Thanks to SIRIM group (AMREC and Shah Alam) and laboratory administrators i.e Pn. Zarina, Mrs. Chanthiriga, Mrs. Helen, En. Hassan and En. Zaharuddin for administrating the labs and equipment.

Special thanks to my fellow colleagues and special friends Hakimeh Wakily, Bashira Shahrudin, Rosma Rohaimi, Edzuwyn Fathin, Fazliny A. Rahman, Rianti Samosir, Nurul Anis Ridzuan, Soleha Shahrudin, Puteri Nur Afiza, Nurul Farah Hana, Nadia Rohaizat, Marhani Che Din, Atiqah Mardziah Mukhtar, Nur Ily Syuhada, Noora Rosli, Fatin Saiha, Siti Mariam, Amir Nawli, Ahmad Najmi, Ahmad Shahril, Zulhilmi Zulkifli, Wan Hafiz, En. Zahari Abdullah, En. Azlai Ta'at, En. Mohd Sani Sa'ayon, En.

Ramlan A. Rahman, Tn. Syed Daud and Mohamed Abdulmunem who made my postgraduate study a wonderful and enriching experience. Also, I am obliged to them who have persistently understanding and supported me throughout my Masters research work.

Last but not least, huge thanks to the contributions of my beloved mama and abah, Che Maznah, Abdul Halim, the twins Fahmi, Farahin for their dua', support, love and trust. Special thanks to Hj. Zaini Abd Ghani, Hjh. Daulath Bibe and family for their endless love and everything. Million thanks to my Makngah and Pakngah, Hjh. Siti Rohani, Ahmad Kamel together with my favourite boy Kautsar Danish, cousins Shafinas Kamel and Shazlina Kamel for their support and wonderful love throughout my study.

Farha Halim

September, 2017.

LIST OF CONTENTS

| | |
|---|----------|
| Title page..... | i |
| Abstract..... | ii |
| Abstrak..... | iv |
| Declaration..... | vi |
| Acknowledgement..... | vii |
| List of contents..... | ix |
| List of figures..... | xiii |
| List of tables..... | xviii |
| List of symbols and abbreviations..... | xix |
| | |
| Chapter 1: Introduction..... | 1 |
| 1.1 Functionally Graded Materials (FGMs)..... | 2 |
| 1.2 Problem Statement..... | 5 |
| 1.3 Aim of the study..... | 7 |
| 1.4 Objectives..... | 8 |
| 1.5 Research Justification..... | 8 |
| | |
| Chapter 2: Literature Review..... | 9 |

| | |
|--|-----------|
| 2.1 Dental Biomaterials..... | 10 |
| 2.2 Dental Post as Medical Devices..... | 11 |
| 2.3 Functionally graded materials (FGMs)..... | 13 |
| 2.3.1 Designation of FGMs as ‘sandwich model’..... | 16 |
| 2.3.2 Heterogeneity of Functionally Graded Material (FGM)..... | 18 |
| 2.4 Titanium and Hydroxyapatite in Functionally Graded Materials (FGMs)..... | 20 |
| 2.4.1 Hydroxyapatite..... | 20 |
| 2.4.2 Titanium..... | 25 |
| 2.5 Coating Titanium Particles with a silica..... | 28 |
| Chapter 3: Materials and Methods..... | 31 |
| 3.1 Preparation of HA and Ti powders..... | 32 |
| 3.2 Synthesis of silica-coated titanium (STP) powder..... | 36 |
| 3.3 Powder Processing Technique..... | 38 |
| 3.3.1 Drying..... | 38 |
| 3.3.2 Milling of the STP Powder..... | 39 |
| 3.4 FGM Fabrication..... | 41 |

| | |
|---|-----------|
| 3.4.1 Compaction using Uniaxial Hydraulic Press..... | 42 |
| 3.4.1.1 Cold Isostatic Press..... | 44 |
| 3.4.2 Sintering..... | 46 |
| 3.5 Characterization Techniques..... | 47 |
| 3.5.1 Morphological Properties..... | 47 |
| 3.5.2 Chemical Properties..... | 47 |
| 3.5.3 Physical Properties..... | 48 |
| 3.5.4 Mechanical Properties..... | 49 |
| Chapter 4: Results..... | 50 |
| 4.1 HA-STP Single Layer..... | 51 |
| 4.1.1 STP Microstructure..... | 51 |
| 4.1.2 Chemical Stability of the HA-STP Single Layer..... | 53 |
| 4.1.3 Vickers' Hardness of the HA-STP Single Layer..... | 57 |
| 4.1.4 Volumetric Expansion of the Sintered HA-STP Single Layer..... | 58 |
| 4.2 FGM Structure..... | 60 |
| 4.2.1 FGM Morphology..... | 60 |
| 4.2.2 Chemical Interaction of HA and STP in the FGM Layers..... | 65 |

| | |
|---|-----------|
| 4.2.3 Vickers' Microhardness of the FGM Layers..... | 66 |
| 4.2.4 Volumetric Expansion of the FGM Layers..... | 67 |
| 4.2.5 Experimental Density of the FGM Layers..... | 68 |
| Chapter 5: Discussion..... | 70 |
| 5.1 STP Synthesis..... | 71 |
| 5.2 Fabrication of the Single-layer Composite..... | 72 |
| 5.2.1 Ti/HA/Si Interactions..... | 72 |
| 5.2.2 Mechanical Performance..... | 75 |
| 5.3 FGM Design..... | 76 |
| 5.3.1 Fabrication Protocol..... | 76 |
| 5.3.2 Chemical analysis..... | 77 |
| 5.3.3 Mechanical Performance..... | 78 |
| Chapter 6: Conclusion..... | 80 |
| 6.1 STP Synthesis..... | 81 |
| 6.2 Fabrication of the FGM Structure..... | 82 |
| Chapter 7: Recommendation for further studies..... | 85 |

| | |
|--------------------------|-----------|
| 7.1 Further studies..... | 86 |
| References..... | 87 |

LIST OF FIGURES

| | |
|---|----|
| Figure 2.1. (a) Diagram of post and core..... | 12 |
| Figure 2.1. (b) Diagram of post and dental crown..... | 12 |
| Figure 2.2. Graphical FGM Representation..... | 18 |
| Figure 2.3. The chemical structure of calcium hydroxyapatite..... | 21 |
| Figure 2.4. Crystalline structure of hydroxyapatite..... | 21 |
| Figure 2.5. Chemical structure of titanium..... | 26 |
| Figure 2.6. Hexagonal crystalline structure of titanium alloy | 27 |
| Figure 3.1. (a) The ball milling machine..... | 34 |
| Figure 3.1. (b) The cups and balls used for milling the HA and Ti powders..... | 34 |
| Figure 3.2 The HA and Ti powders after grinding in the ball mill machine..... | 35 |
| Figure 3.3. Experimental setup for synthesizing silica-coated titanium (STP)..... | 36 |
| Figure 3.4. Stirring of titanium powder at 800 rpm for 4 hours..... | 37 |
| Figure 3.5. Initial suction of the unattached silica by a pipette..... | 38 |
| Figure 3.6. The oven used to dry HA, Ti and STP powders..... | 39 |

| | |
|---|----|
| Figure 3.7. (a) HA and STP powders before mixing | 40 |
| Figure 3.7. (b) Homogeneous mixing of HA-STP using ceramic mortar | 40 |
| Figure 3.8. Schematic illustration of multilayered and composition of each layer HA-STP of the fabricated specimens..... | 41 |
| Figure 3.9. (a) The flexible plastic tube..... | 42 |
| Figure 3.9 (b) The lubricant materials..... | 42 |
| Figure 3.10. Schematic of the method used to flatten the FGM layers with a gentle pressure using plunger..... | 43 |
| Figure 3.11. Compaction of green FGM specimen by hydraulic press machine..... | 43 |
| Figure 3.12. (a) Cold isostatic press machine..... | 44 |
| Figure 3.12. (b) The rubber glove used to protect the specimens from contamination by the CIP oil..... | 45 |
| Figure 3.13. (a) The sintering furnace..... | 46 |
| Figure 3.13. (b) The sintering cycle..... | 46 |
| Figure 3.14. A typical FGM specimen after sintering..... | 46 |
| Figure 3.15. The X-ray diffraction machine..... | 48 |
| Figure 3.16. The microhardness testing machine..... | 49 |
| Figure 4.1. (a) The microscopic image of Ti..... | 51 |

| | |
|---|----|
| Figure 4.1. (b) The microscopic image of STP..... | 51 |
| Figure 4.2. The EDX analysis of the STP powder..... | 52 |
| Figure 4.3. (a) The XRD analysis of titanium (Ti)..... | 54 |
| Figure 4.3. (b) The XRD analysis of silica-coated titanium (STP)..... | 54 |
| Figure 4.3. (c) The XRD analysis of sintered HA-Ti..... | 54 |
| Figure 4.3. (d) The XRD analysis sintered of HA-STP..... | 54 |
| Figure 4.4. (a) The FT-IR spectra of HA..... | 55 |
| Figure 4.4. (b) The FT-IR spectra of STP..... | 55 |
| Figure 4.4. (c) The FT-IR spectra of calcinated HA-STP..... | 55 |
| Figure 4.4. (d) The FT-IR spectra of sinteredd HA-Ti..... | 55 |
| Figure 4.4. (e) The FT-IR spectra of sintered HA_STP..... | 55 |
| Figure 4.5. Comparison between the Vickers' hardness values of the sintered pure titanium, Ti3-HA, HA-Ti, and HA-STP composite..... | 57 |
| Figure 4.6. Comparison between the expansion ratios of sintered pure titanium, Ti3-HA, HA-Ti, and HA-STP composite..... | 58 |
| Figure 4.7. (a) The sintered FGM structures using pure Ti..... | 59 |
| Figure 4.7. (b) The sintered FGM structures using STP..... | 59 |
| Figure 4.8. (a) SEM Micrographs and elemental analyses of 9STP-1HA..... | 61 |

| | |
|--|----|
| Figure 4.8. (b) SEM Micrographs and elemental analyses of 8STP-2HA..... | 61 |
| Figure 4.8. (c) SEM Micrographs and elemental analyses of 7STP-3HA..... | 62 |
| Figure 4.8. (d) SEM Micrographs and elemental analyses of 6STP-4HA..... | 62 |
| Figure 4.9. (a) The peak intensities of Ti, Si, Ca, and P elements in 9STP-1HA layers of FGM structure..... | 63 |
| Figure 4.9. (b) The peak intensities of Ti, Si, Ca, and P elements in 8STP-2HA layers of FGM structure..... | 63 |
| Figure 4.9. (c) The peak intensities of Ti, Si, Ca, and P elements in 7STP-3HA layers of FGM structure..... | 63 |
| Figure 4.9. (d) The peak intensities of Ti, Si, Ca, and P elements in 6STP-4HA layers of FGM structure..... | 63 |
| Figure 4.10. (a) The XRD spectra of different FGM layer of STP..... | 64 |
| Figure 4.10. (b) The XRD spectra of different FGM layer of 9STP-1HA..... | 64 |
| Figure 4.10. (c) The XRD spectra of different FGM layer of 8STP-2HA..... | 64 |
| Figure 4.10. (d) The XRD spectra of different FGM layer of 7STP-3HA..... | 64 |
| Figure 4.10. (e) The XRD spectra of different FGM layer of 6STP-4HA..... | 64 |
| Figure 4.11. Comparison between the Vickers' hardnesses of different FGM layers..... | 67 |

Figure 4.12. Comparison between the volumetric expansion of different

FGM layers.....68

Figure 4.13. The experimental densities of different FGM layers and

STP-HA composite.....69

University of Malaya

LIST OF TABLES

| | |
|--|----|
| Table 2.1. (a) Crystallographic properties: Lattice parameters ($\pm 0.003 \text{ \AA}$)..... | 22 |
| Table 2.1. (b) Chemical and structural comparison of teeth, bone and hydroxyapatite (HA)..... | 22 |
| Table 3.1. Physical and chemical properties of green powders..... | 33 |
| Table 3.2. Specification of solutions in the study..... | 33 |

LIST OF SYMBOLS AND ABBREVIATIONS

| | | |
|-------------------------|---|------------------------------|
| Å | : | Armstrong |
| nm | : | nanometer |
| a.u. | : | arbitrary unit |
| 2θ | : | 2-theta |
| HV | : | Vickers' hardness |
| FE | : | Finite element |
| EF | : | Electric furnace |
| α | : | Alpha |
| β | : | Beta |
| α -TCP | : | Alpha tricalcium phosphate |
| β -TCP | : | Beta tricalcium phosphate |
| bcc | : | body-centered cubic |
| hcp | : | hexagonal close-packed |
| Ti | : | Titanium |
| HA | : | Hydroxyapatite |
| HA-Ti | : | Hydroxyapatite – titanium |
| STP | : | Silica-coated titanium |
| FGM | : | Functionally graded material |
| Ca_xP_y | : | Calcium phosphate |
| CaSiO_3 | : | Calcium silicate |

| | | |
|-------------------------|---|-------------------------|
| CaTiO_3 | : | Calcium titanate |
| CaCO_3 | : | Calcium carbonate |
| CO_2 | : | Carbon dioxide |
| CaO | : | Calcium oxide |
| SiO_2 | : | Silica |
| TTCP | : | Tetra calcium phosphate |
| TCP | : | Tricalcium phosphate |
| Ti_xP_y | : | Titanium phosphides |
| Ti_xO_y | : | Titanates |
| TEOS | : | Tetraethylorthosilicate |
| HCl | : | Hydrochloric acid |
| H_3PO_4 | : | Hydrophosphoric acid |
| CIP | : | Cold isostatic press |
| HIP | : | Hot isostatic press |
| SPS | : | Spark plasma sintering |
| PM | : | Powder metallurgy |

Chapter 1

Introduction

1.1 Functionally Graded Materials (FGMs)

The restoration of endodontically treated teeth is a challenging task because it usually involves the treatment of teeth with significant loss of tooth structure (Abu Kasim *et al.*, 2011). Biomedical-graded metallic compounds such as titanium, stainless steel, and their alloys are potential components for fabrication of load-bearing implants due to their favourable mechanical behavior. The facile chemical and surface modification of these compounds also allows altering various biological and physical properties according to their intended application. However, a crucial limitation of the metallic implants is their significantly higher rigidity in contrast to the bone/tooth structure, which results in stress concentration in interfaces during loading, leading to the catastrophic fracture of the bone/tooth tissue. The existence of tooth fracture has been described as a major failure for endodontically treated teeth, and is the third most common cause of tooth loss after dental caries and periodontal disease. A potential solution to moderate the mechanical properties of these metallic alloys is incorporation of biocompatible and bioactive ceramics with similar mechanical behavior to the bone/tooth structure.

It is also important to note that because of the gradient nature of bone/tooth structure, the mechanical properties at different regions of these tissues are not identical. Therefore, application of homogeneous implants within these heterogeneous structures results in stress concentration in regions where the mechanical properties of the implant is significantly different than those of bone/tooth tissue. In order to overcome this challenge, design and development of functionally graded structures for improving the mechanical performance of biomaterials has recently received increasing attention in material science. FGMs are a new class of advanced composites that comprised of several continuous, or discontinuous layers, gradient in composition and microstructure (Shahrjerdi *et al.*, 2011). FGMs are promising components for fabrication of dental

implants and dental posts. FGMs can mimic the bone properties without compromising on the mechanical properties of the materials. The gradient functions in mechanical properties and biomechanical affinity to tooth structure, contribute to the efficient biocompatibility (Cao and Hench, 1996). These results in gradient tissue reaction in response to the graded structure of FGM, which implies the possibility to control the tissue response through the gradient function of FGM (Watari *et al.*, 2004). When used as biomaterials, FGMs must simultaneously satisfy many requirements such as non-toxicity, corrosion resistance, thermal conductivity, mechanical strength, fatigue durability, biocompatibility, and aesthetics (Hedia and Mahmoud, 2004).

A number of fabrication methods have been invented to fabricate load-bearing functionally graded implants for dental and orthopedics applications. These FGMs are mostly composed of biomedical-graded metallic alloys such as titanium (Ti) or stainless steel as well as biocompatible and bioactive ceramics such as hydroxyapatite (HA), zirconia, silica, and bioactive glass.

Silica, which is a stable oxide of silicon (SiO_2), is a bioactive material with high corrosion resistance. Carlisle (1970) established a biological basis for the role of silica in bone formation. Silica is thought to perform a specific metabolic function that partake in cellular development and gene expression (Hing *et al.*, 2006). Secondly, the existence of chemical functions in the silica structure could enhance the precipitation of an apatite layer on the surface of bioactive materials. The silica particles can improve the strength of HA coatings by particle mediated reinforcement, leading to crack deflection or crack arrest. Therefore, silica is believed to play a critical role in bioactive materials by acting as a cross-linking agent in connective tissue, providing sufficient integration with the bone structure (Morks *et al.*, 2008, Sadjadi *et al.*, 2011). The amorphous SiO_2 is a promising candidate to enhance the mechanical properties of hydroxyapatite (HA)

coatings; however, pure SiO₂ cannot be used for load-bearing applications because of its poor mechanical properties compared to natural bone. However, incorporation of silica in Ti-based FGMs may allow obtaining both biocompatibility and mechanical stability in resulting implants. SiO₂ and Ti provide reinforcement via increasing the bonding strength of HA particles and abrasion resistance (Morks *et al.*, 2008).

HA [Ca₁₀(PO₄)₆(OH)₂] is another potential bioceramic which can be incorporated in FGM structures due to its bioactivity and *in vivo* osteo-conductive properties (Chenglin *et al.*, 1999, Watari *et al.*, 1997). A wide variety of substitutions for Ca²⁺, PO₄³⁻, and/or OH⁻ ions could be incorporated in the HA chemical structure. However, the poor mechanical properties of HA as compared to natural bones, especially the low tensile strength and fracture toughness, significantly restrict its direction application as load-bearing implants, such as hip-joints, tooth roots, and femur bones (Ye *et al.*, 2009). Therefore, fabrication of FGM structures using metallic compounds (especially Ti-based alloys) and HA could be an effective approach to offer both mechanical strength and biocompatibility contributed by Ti and HA, respectively. Ti alloy have superior mechanical properties which make them withstand load bearing applications (Morks *et al.*, 2008). Abu Kasim *et al.* (2011) showed that dental posts with functionally graded structure could provide superior performance compared to traditional homogeneous and uniform materials. Ideally, this dental post should stabilize the core and not weaken the tooth. It has been suggested that a post should only be used when the remaining coronal tooth tissue can no longer provide adequate support and retention for restoration (Assif *et al.*, 1993, Torbjörner and Fransson, 2004). But, in the past it was thought that posts reinforced endodontically treated teeth (Abu Kasim *et al.*, 2011, Silverstein, 1964), however, other studies have shown otherwise as a post may be a predisposing factor for root fracture (Hunter *et al.*, 1989, Peroz *et al.*, 2005).

The development of new biomaterials with enhanced mechanical properties and biocompatibility has become a major challenge in biomaterials community. This new biomaterials enhancement towards the upgrading for functionally graded materials which is the new approach for the improvement of dental post material performance compared to traditional homogeneous and uniform materials (Watanabe *et al.*, 2002). It is also important to note that because of the gradient nature of bone/tooth structure, the mechanical properties at different regions of these tissues are not identical. Therefore, application of homogeneous implants within these heterogeneous structures results in stress concentration in regions where the mechanical properties of the implant is significantly different than those of bone/tooth tissue. In order to overcome this challenge, design and development of functionally graded structures for improving the mechanical performance of biomaterials has recently received increasing attention in the material science. FGMs are a new class of advanced composites that comprised of several continuous or discontinuous layers, gradient in composition and microstructure (Shahrjerdi *et al.*, 2011).

1.2 Problem Statement

Ti and HA are the most studied materials for producing FGM composites layer. By utilizing the FGM structures in biomedical application, it can simulate the gradient mechanical properties of bone structure by fabricating various layers with different metallic-ceramic weight ratios. Furthermore, the Ti-HA composites exhibit characteristics such as bio-inertness, a low Young's modulus, and high biocompatibility. However, the undesirable interaction of HA and Ti during the sintering process results in composites with poor mechanical characteristics (Arifin *et al.*, 2014, Xiao *et al.*, 2005). Pure HA dehydroxylate at approximately 900 °C in air and at 850 °C in a water-free

atmosphere, followed by decomposition of Tetra calcium phosphate (TTCP: $\text{Ca}_4(\text{PO}_4)_2\text{O}$) and/or Tricalcium phosphate (TCP: $\text{Ca}_3(\text{PO}_4)_2$) (Arifin *et al.*, 2014). However, during the sintering of HA-Ti systems, Ti ions react with the dehydrated water of HA to yield titanium oxide, thereby accelerating the dehydroxylation and decomposition of HA (Arifin *et al.*, 2014). Based on the experimental parameters, the sintering products might include TCP, TTCP, calcium titanate (CaTiO_3), titanium phosphides (Ti_xP_y), titanates (Ti_xO_y), calcium oxide (CaO), and amorphous phases (Yang *et al.*, 2004). Particularly under argon atmosphere, it is reported that at 1200 °C, the calcium phosphate phases were completely eliminated from the composite and the titanium/titanate particles were covered with a compact layer of Ti_xP_y and CaTiO_3 phases (Balbinotti *et al.*, 2011).

It is well-known that the mechanical behavior of the HA-Ti system is significantly affected by the microstructure and phase distribution in the sintered composite. Previous studies indicated that some phases such as Ti_xP_y and CaTiO_3 which form between titanium and HA particles at elevated temperatures, present a fragile behaviour without displaying any yield stress prior to the rupture and thus provide weak interface bonding in the matrix. These fragile phases are consequently removed during polishing, resulting an uneven appearance with gaps and pores between titanium particles (Balbinotti *et al.*, 2011). One particular approach to address this issue, is the incorporation of low-melting-point biocompatible additives as a sintering aids to the initial components (Ning and Zhou, 2008). However, this approach may not eliminate the undesired sintering products especially in composites with high HA/Ti ratios.

Wakily *et al.*, (2015) presented a new technique for improving the thermal and mechanical properties of Ti-HA composites with high Ti/HA ratios in recent publication. In this approach, the Ti particles were coated by thin silica layers prior to mixing with HA to prevent the undesired metallic-ceramic reactions at increased temperatures. By

removing the fragile compounds, the resulting composite may provide improved mechanical strength for load-bearing application.

In the literature, it was found that the HA/Ti FGMs with symmetrically distributing compositional profiles pre-designed, have always many microcracks on the surfaces because of unjustified distribution of the residual thermal stress during the fabrication process, which can deteriorate the properties of FGM (Chu *et al.*, 2001). The poor interfacial bonding at metallic-ceramic interface is another challenge which occurs because of the layer-by-layer fabrication of FGM structures (Watari *et al.*, 1997). Guo and Noda (2007) indicated a crack formation and propagation along interfaces due to the large differences in fracture strengths of FGM layers. Fabrication of gradient structures as alternative to the layer-by-layer FGMs may be a particular strategy to reduce the risk of sudden toughness change along the material interface and decrease the risk of crack propagation. Therefore, in this work we will also modify the previous fabrication method to eliminate the layer interfaces and obtain a gradient structure, which may result in reduced crack formation and propagation within the material.

1.3 Aim of the Study

The aim of the present study is to improve the physical and mechanical properties of functionally graded materials made from hydroxyapatite and titanium by decreasing the undesirable metallic-ceramic interactions.

1.4 Objectives

1. To investigate the effect of surface modification of titanium particles by a silica protective layer on the physical, chemical and mechanical properties of hydroxyapatite-titanium composites.
2. To fabricate and characterize a new type of functionally graded material (FGM) using hydroxyapatite (HA) and silica-coated titanium (STP).

1.5 Research Justification

In this study, silica was used to act as a protective layer to reduce the physical and chemical reactions between the main FGM constituents. The benefit of Ti coated with silica particle include enhanced colloidal stability, potential for enhanced interfacial bond formation when used with silane coupling agents in nanocomposite development, and enhanced bioactivity due to the established role of silica in bond formation. The fabrication of a new type of functionally graded material is modified where the materials will be pressed in one step rather than layer-by-layer pressing.

Chapter 2

Literature Review

2.1 Dental Biomaterials

This chapter discusses metal-ceramics biomaterials and functionally graded biomaterials for the application of dental post in the prosthodontic. Modern types of the metal-ceramic biomaterials have become the main challenge of future research used to substitute the metals, glass-ceramics and sintered ceramics for dental restorations (Höland *et al.*, 2009). In the dental biomaterials, it is believed to have a highly aesthetic appearance that is comparable to that of natural teeth. Several variables contribute to the long-term success of restorations have been presented along with a brief review of the physics, chemistry, and mechanical underlying the operation mechanism of these metal-ceramic biomaterials and optimization of a novel functionally graded materials fabrication in the oral environment. Evaluation of the comprehensive characteristics on the mechanical properties of new dental materials such as elastic properties, hardness, dynamic mechanical properties (visco-elasticity) and fracture mechanical properties were reviewed to provide complete understanding of the mechanical properties of human teeth (Zhang *et al.*, 2014).

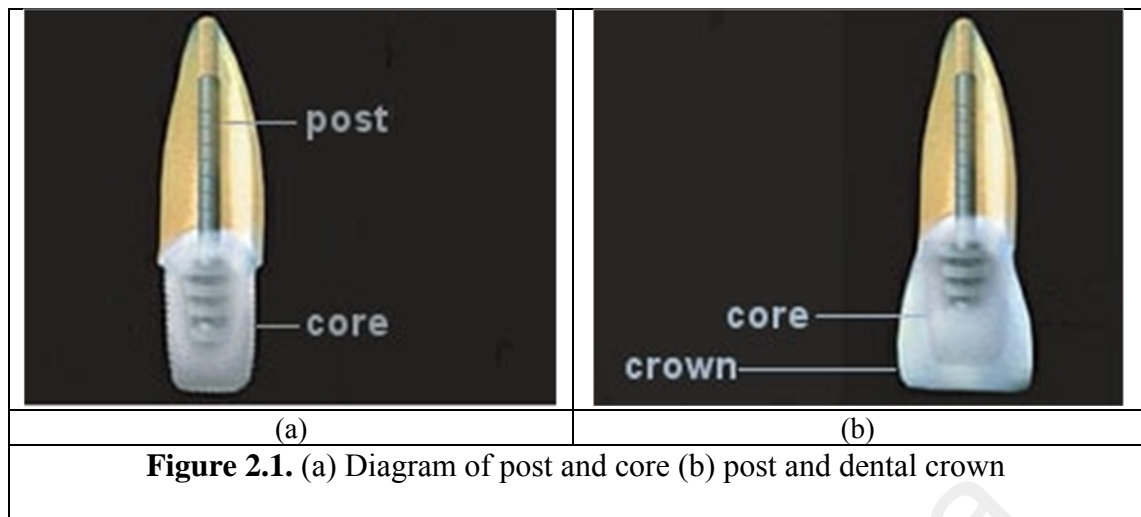
The special focus on a crucial limitation of the metallic implants that is significantly higher rigidity in contrast to the bone or tooth structure, which results in stress concentration in interfaces during loading, leading to the catastrophic fracture on the bone or tooth tissue. At this point, the important aspects which need to be considered is the potential solution to moderate the mechanical properties of these metallic alloys with incorporation of biocompatible and bioactive ceramics with similar mechanical behaviour to bone or tooth structure (Bruschi *et al.*, 2015). The trend has emerged towards implant-supported restorations, particularly in the replacement of single teeth. Metal-ceramic materials has to be emphasized to the success of biomaterials in human medicine

which is determined by the long-term clinical expectations and development of longer life expectancy (Höland *et al.*, 2009).

2.2 Dental posts as Medical Devices

The process of biomaterial or medical device innovations are driven by clinical needs. The basic dental materials were known as implants and considered suitable to replace natural tissue when it had minimal or zero toxicity (Arifin *et al.*, 2014, Shirtliff and Hench, 2003). The roughness of an implant surface is conducive to the bonding between implant materials and tissues. Biomaterials should possess properties such as non-toxicity, corrosion resistance, thermal conductivity, strength, fatigue durability, biocompatibility and sometimes aesthetics (Sadollah and Bahreininejad, 2012). Furthermore, in the most fundamental activity of human beings, dental implant is potentially used for restoring the function of chewing and biting, and therefore eating (Sadollah and Bahreininejad, 2012).

A dental post is placed after root canal treatment of a crown (Peroz *et al.*, 2005) and to resist vertical dislodging forces (Schwartz and Robbins, 2004). When it has provided sufficient retention to the final restoration, it showed acceptable fracture resistance and protecting the remaining tooth. The structure of post and core are divided into two parts; the post and the core. The post is determined by a small rod, usually metal, ceramic or fiber reinforced posts, that is cemented after a successful root canal treatment (Sidoli *et al.*, 1997). The post is then used to hold the core, or a filling in place. The schematic diagram of a post is shown in the Figure 2.1(a-b).



Another part is the core, replaces missing tooth structure in preparation for making a new dental crown. The core utilized to hold a dental crown in place that can be directly built up from dental materials, such as composite or amalgam. A dental post can be used to help to hold the core to the tooth (Fernandes and Dessai, 2001).

The benefits of dental posts which are often casted or prefabricated from homogeneous materials such as stainless steel, titanium, gold, chromium-cobalt alloys, fiber, and zirconium resulted in high success rates in improving the fracture resistance of the endodontically-treated teeth. However, the increased risk of vertical fracture in the teeth restored by ceramic and metallic posts occurred due to their high elastic moduli compared to natural dentine (Abdulmunem *et al.*, 2015). Studies showed that the dental posts do not reinforce the endodontically treated teeth (Heydecke *et al.*, 2001). The existence of surface flaws and defects have weakened crowns under stress (King and Setchell, 1990, Ottl *et al.*, 2002).

In case of considerable hard tissue loss, posts are used as an element supporting core foundation when there is insufficient coronal tooth structure. Most of clinicians choose the post and core system which provides best retention, support, and reduces the possibility of root fracture (Al-Wahadni *et al.*, 2008). In the selection of post material, the

common considerations are usually based on its biocompatibility, mechanical properties, ease of fabrication, and availability in the market and cost factor (Helal and Shi, 2016).

Post retention refers to the ability of a post to resist vertical dislodging forces. Post retention are influenced by the post parameters; post's length, design, diameter, post fitting and the luting cement used, tooth type and its position and ferrule effect. The increase in post length can increase the retention whereby the design of a post:- parallel posts are more retentive than tapered posts (Richard *et al.*, 2004). In previous studies, an increase in post width has no significant effect on its retention and the influence of post width also revealed that the tooth restored with larger diameter posts provide the least resistance to fracture with a decrease in the width of the remaining dentine (Fernandes *et al.*, 2003, Trabert *et al.*, 1978).

2.3 Functionally graded materials (FGMs)

The idea of functionally graded materials (FGMs) was advanced substantially in the early 1980's in Japan, where this new material concept was been proposed to increase adhesion and to minimize the thermal stresses in metallic-ceramic composites developed for reusable rocket engines (Gupta and Talha, 2015). Structures of FGMs are not simply inhomogeneous, but their heterogeneity would be typical in one direction for the entire volume of a material. It is characterized by a gradual change in material properties over volume and had a promising approach for bone tissue repair (Zhou *et al.*, 2015). FGMs are high performance, microscopically inhomogeneous materials with engineered gradients of composition and specific structure in the preferred orientation (Gupta and Talha, 2015).

Continuous changes in their microstructure make FGMs distinct from other traditional composite materials which fail through a process called delamination in the extreme mechanical and thermal loadings. The commonly available FGMs are ceramic-metal composites, where the ceramic part has good thermal and corrosion resistance capability and metallic part provide superior fracture toughness and weldability (Gupta and Talha, 2015). Howard *et al.*, (1994) have found that the FGM can act as an interface layer to connect two incompatible materials to enhance the bond strength, remove stress concentration, provide multifunctional, ability to control deformation, dynamic response and wear corrosion.

FGM also can decrease the magnitude of the peak thermal stress concentrations at the interface layers and free edges in laminated composites. An introduction of metallic phase that deforms plastically in FGM improves the fracture toughness of brittle ceramics (Erdogan, 1995, Shaw, 1998). Ultimately, one of the processing methods of FGMs can be classified into a category which is based on the constructive processing and mass transport when FGM is constructed layer-by-layer starting with an opposite distribution in which the gradients are literally constructed in space. These whole processes results in advantage to fabricate unrestricted number of gradients (Gupta and Talha, 2015).

The existence of tooth fracture has been described as a major failure for endodontically treated teeth, and is the third most common cause of tooth loss after dental caries and periodontal disease. A potential solution to moderate the mechanical properties of these metallic alloys is incorporation of biocompatible and bioactive ceramics with similar mechanical behavior to the bone or tooth structure. The introduction and advancement of composite materials and functionally graded materials enable researchers to be integrated in a wide range in choice of selection of materials for different applications with good efficiency.

The benefits FGMs are due to their many features considered useful for application in the biomedical applications. For an example, the gradual transition in microstructure or compositions in the composites, ‘smoothing’ the transition for reduction of thermal stress, to minimize or eliminate the stress concentration and tailored the functional performance of gradually materials (Obbineni, 2013). FGMs offer great agreement in applications where high amount of ceramic materials or pure ceramic is needed to arrange at the upper face at high temperature conditions, corrosive environment, which is in the same way high amounts of metal are provided.

In order to overcome this challenge, design and development of functionally graded structures for improving the mechanical performance of biomaterials has recently received increasing attention in the material science. FGM is known as a new class of advanced composites that comprised of several continuous or discontinuous layers, gradient in composition and microstructure (A. Shahrjerdi *et al.*, 2011).

FGMs are promising components for fabrication of dental implants and dental posts. FGMs can mimic the bone properties without compromising on the mechanical properties of the materials. The gradient functions in mechanical properties and biomechanical affinity to tooth structure, contribute to improved biocompatibility (Cao and Hench, 1996). These results in gradient tissue reaction in response to the graded structure of FGM, which implies the possibility to control the tissue response through the gradient function of FGM (Watari *et al.*, 2004). When used as biomaterials, FGMs must simultaneously satisfy many requirements such as non-toxicity, corrosion resistance, thermal conductivity, mechanical strength, fatigue durability, biocompatibility, and aesthetics (Hedia and Mahmoud, 2004).

A number of fabrication methods have been invented to fabricate load-bearing functionary graded implants for dental and orthopedics applications. These FGMs also

mostly composed of biomedical-graded metallic alloys such as Ti or stainless steel as well as biocompatible and bioactive ceramics such as HA, zirconia, silica, and bioactive glass. The fabrication of titanium-silica FGM for dental application was carried out (Besinis *et al.*, 2014). This new biomaterials enhancement towards the upgrading for functionally graded materials which is the new approach for the improvement of dental post material performance compared to traditional homogeneous and uniform materials (Watanabe *et al.*, 2002). It is also important to note that because of the gradient nature of bone or tooth structure, the mechanical properties at different regions of these tissues are not identical.

Therefore, application of homogeneous dental post within these heterogeneous structures results in stress concentration in regions where the mechanical properties of the implant is significantly different than those of bone or tooth tissue. In order to overcome this challenge, design and development of functionally graded structures for improving the mechanical performance of biomaterials has recently received increasing attention in the material science. The properties of FGMs change from one surface to another according to a smooth or continuous function based on the position throughout the thickness of the material respectively (Miyamoto *et al.*, 2013).

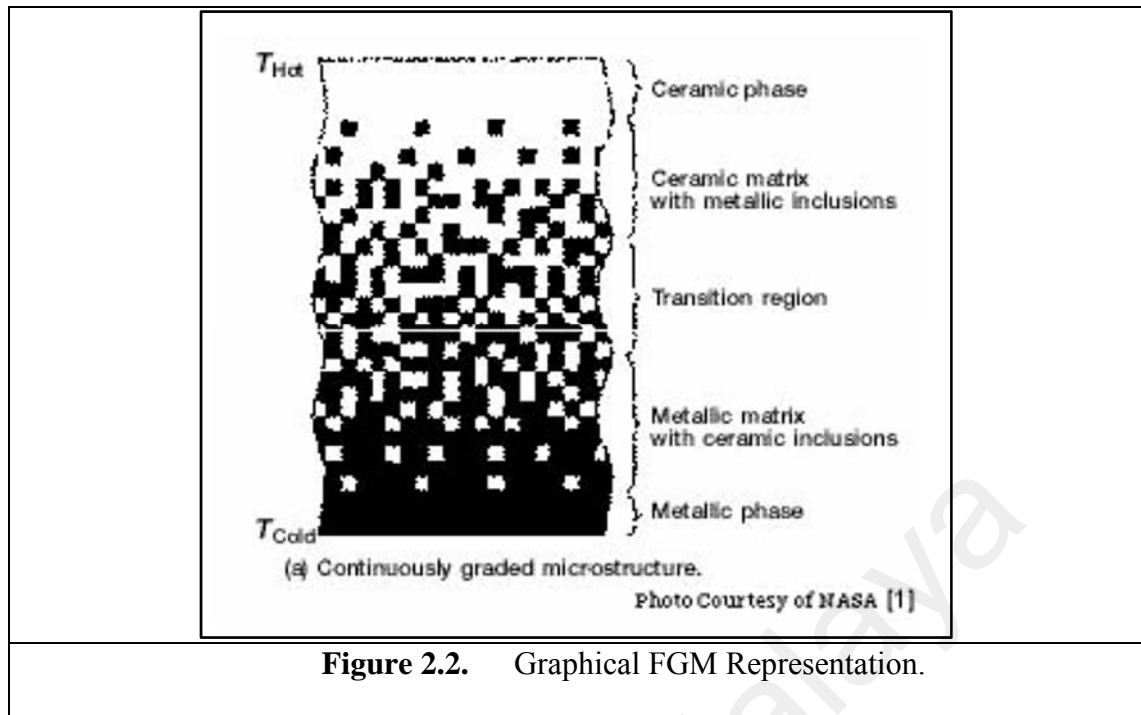
2.3.1 Designation of FGMs as ‘sandwich model’

Researchers have been utilizing the exciting prospects of the functionally graded dental material in the domain of so called ‘sandwich model’ which sandwich beam is going to be used in recent work. The introduction and advancement of composite materials and functionally graded materials enable researchers to be integrated in a wide range in choice of selection of materials for different applications with good efficiency. There are features of FGM which considered to be extended to other application in the

biomedical applications; the gradual transition in microstructure or compositions in the composites, 'smoothing' the transition for reduction of thermal stress, to minimize or eliminate the stress concentration and tailored the functional performance of gradually materials to be integrated in a wide range of applications (Obbineni, 2013). These graded ceramic-metal FGMs are best example for high temperature environmental conditions and in the oral environment.

The pace of development properties of FGMs made them more suitable for specific applications as face layers of sandwich structure. The potential of material in one surface maintains the homogeneous material property of ceramic and metal. The FGMs offer great agreement in applications where high amount of ceramic material or pure ceramic is needed to arrange at the upper face at high temperature conditions, corrosive environment, in the same way high amounts of metal are provided (Obbineni, 2013).

In 1984, Japanese material scientists first explored this concept in order to develop thermal barrier materials and to create high-performance heat-shielding ceramic-based composites for structural components in aerospace applications (Mahamood *et al.*, 2012). An addition of a FGM layer between the ceramic and the cement, and investigate the effect of the FGM layer, which is inspired from the initial grading by measurements of modulus variations across the dentin-enamel junction (Huang *et al.*, 2007). The material transitions from a metal to a ceramic by increasing the percentage of ceramic material present in the metal until the appropriate percentage is reached or a pure ceramic is achieved. Figure 2.2 showed the graphical FGM representation of metallic-ceramic transition (Chapman, 2006).



The bulky specimens in FGMs with strong interfacial bonding and reduced thermal stresses unlike coatings on substrates. For an example, the fabrication of functionally graded tricalcium phosphate/fluoroapatite composites and later prepared to combine the bioactive fluoroapatite with the bioresorbable tricalcium phosphate (Wong *et al.*, 2002). Fundamentally, the combination of mechanical properties and biocompatibility are very important factors in application of any biomaterial to medical or dental fields. Based on previous studies, the combination of HA and Ti-6Al-4V phase can form an excellent FGM by exhibiting excellent biocompatibility and bone-bonding ability or dental-bonding ability and improved mechanical strength in the FGM (Khor *et al.*, 2003).

2.3.2 Heterogeneity of Functionally Graded Materials (FGMs)

It is well known that the intended biocompatibility and osseointegration can be improved from an optimized mechanical behaviour of functionally graded (Chu *et al.*,

2006, Sadollah and Bahreininejad, 2012). In general, FGM is believed to be applied as a new kind of heterogeneous materials and composites materials for the application of material physics/dental materials. FGM is a kind of inhomogeneous body, which characterized at different areas of the material, the mechanical properties of the material show a gradient continuous change between interfaces and it can be controlled (S. Cheng, 2015, Z. Cheng *et al.*, 2015).

The surface of teeth are composed of hard enamel with prismatic HA crystallite, whereas the internal core composed of dentine with collagen fibrils and HA. Since enamel has shown as hard and extremely wear resistant, however the internal part is relatively soft and flexible in the functionally graded structures of teeth. This transition from enamel to dentine is provided by the intermediate layer, where the composition gradually transitions from one material to the other (Chen and Fok, 2014, Sola *et al.*, 2011). When a functionally graded dental post with similar heterogeneity to the tooth structure is fabricated, a less risk of root fracture is expected due to the better mechanical match at post-dentine interfaces.

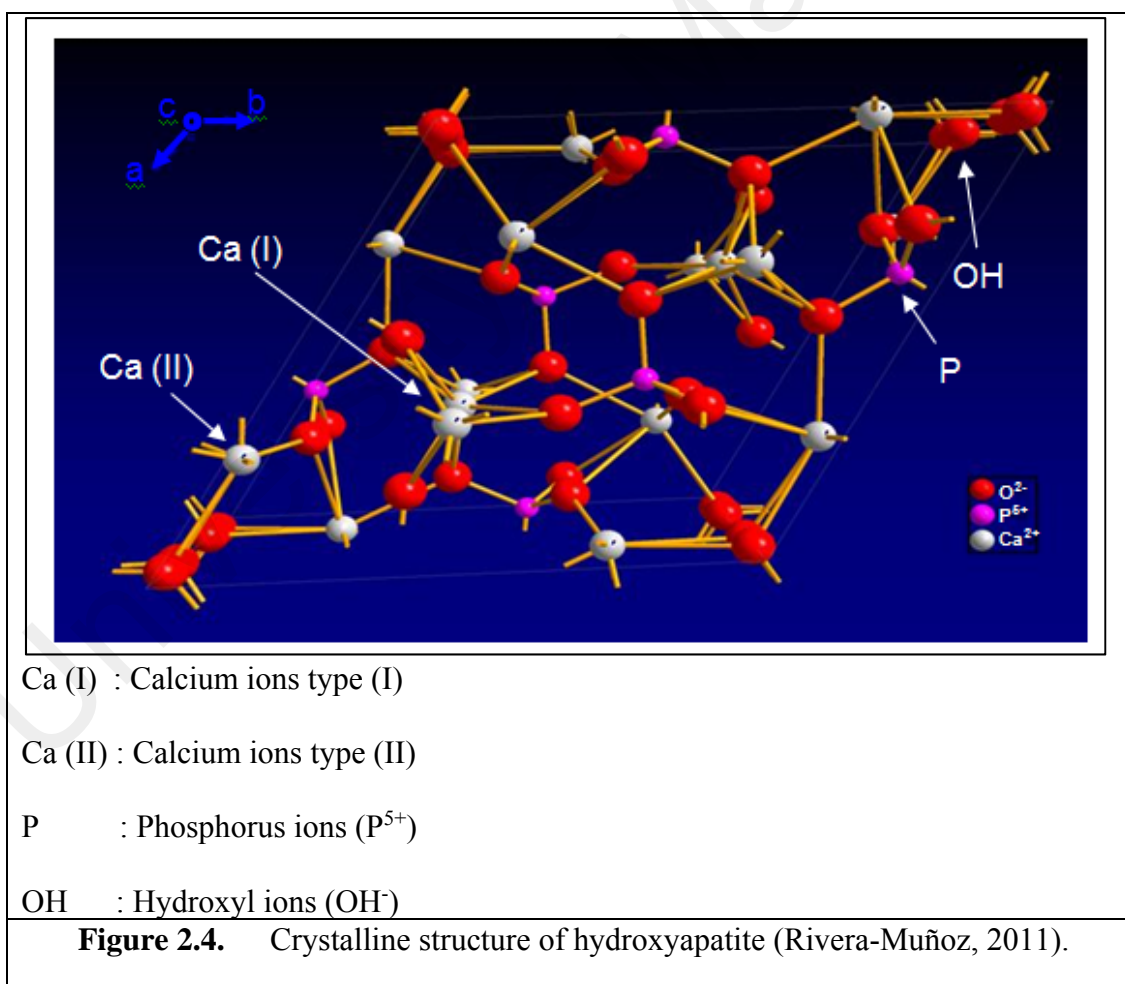
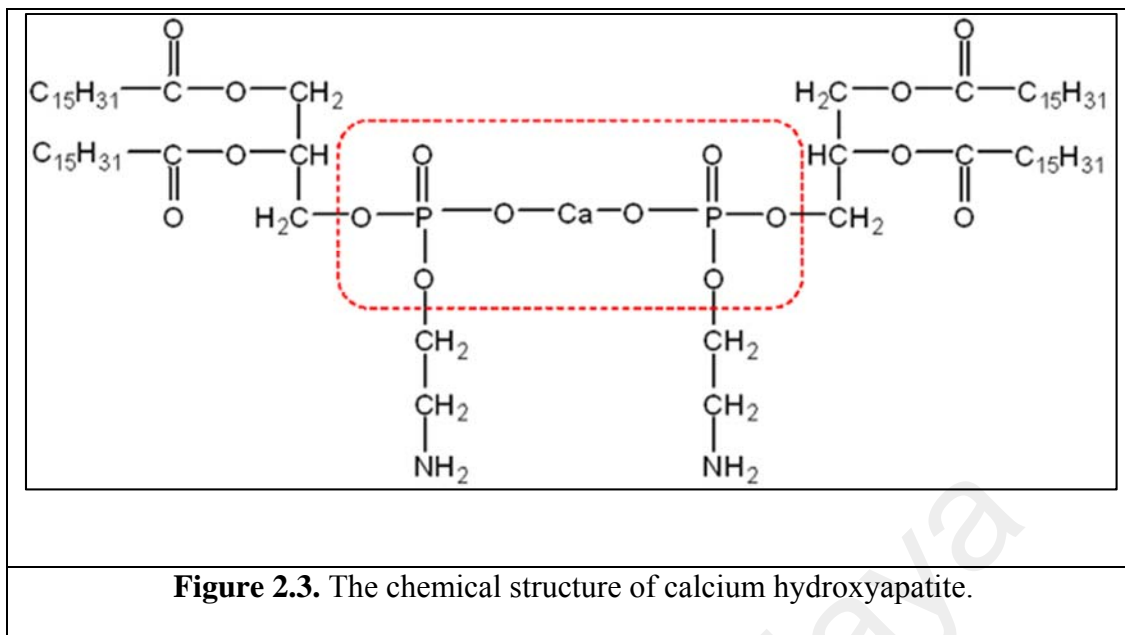
Due to the mechanical behaviour, it is important to ascertain the thermal behaviour of FGDPs in order to obtain a more realistic prediction to their performance in the oral environment. Kumar and Wang, (2002) reported that step-wise or continuously graded metal-ceramic composites are designed to improve interfacial bonding between dissimilar solids, to minimize and optimally distribute thermal stresses, to suppress the onset of plastic yielding and reduce the effective driving force for fracture together with arrest crack. Despite all the propagation properties, by designing FGM, it can lower the internal stresses and crack length of the graded and layered structures will be computed. FGM layer resulted as gradually decreases of Young's modulus from that of the dental ceramic to a lower value (Huang *et al.*, 2007).

2.4 Titanium and Hydroxyapatite in Functionally Graded Materials (FGMs)

The teeth surfaces are composed of hard enamel with prismatic HA crystallite, whereas the internal core composed of dentin with collagen fibrils and HA. This transition from enamel to dentine is provided by the intermediate layer, where the composition gradually transitions from one material to the other (Chen and Fok, 2014, Sola *et al.*, 2011). Functionally graded dental post composed of titanium (Ti) and hydroxyapatite (HA) with similar heterogeneity to the tooth structure have shown potential to reduce the risk of root fracture due to their better mechanical match at post-dentine interfaces.

2.4.1 Hydroxyapatite

Hydroxyapatite (HA) with the formula $\text{Ca}_{10}(\text{PO}_4)_6(\text{OH})_2$ is another potential bioceramic and most documented was the calcium phosphate ceramic (Figure 2.3). Theoretically, HA exists as hydroxyl end-member of apatite which was suggested in 1912 (Arifin *et al.*, 2014). HA can be used in bulk form or as a coating material due to its bioactivity and in-vivo osteoconductive properties which highly incorporated in functionally graded material structures (Chenglin *et al.*, 1999, Watari *et al.*, 1997) and biomaterial of choice in both dentistry and orthopaedics (Sakkers *et al.*, 1997). Its composite are also known as promising materials for manufacturing of the load-bearing implants (Wakily *et al.*, 2015). HA is one of the apatite structures that were observed in rock and has main crystalline component of the mineral phase in bone and teeth (Rivera-Muñoz, 2011). The structure similarities between HA, enamel, dentine and bone makes it the most clinically used as biomaterial for medical and dental applications (S.V. Dorozhkin and Epple, 2002).



In addition, a wide variety of substitution for Ca^{2+} , PO_4^{3-} , and/or OH^- ions as in Figure 2.4 could be incorporated in the HA chemical structure. HA as an implant can bond and promote natural tissue growth with supporting cell fate process due to its similarity to bone mineral (Chang *et al.*, 2000, Ruys *et al.*, 1995, Tampieri *et al.*, 2000). In the structure of HA, it has a hexagonal symmetry and unit cell lattice parameters, $a = 0.94$ nm and $c = 0.68$ nm. Every unit cell in HA is considered to be arranged along c-axis, as lattice parameters and its symmetry are taking into consideration. From here, a preferred orientation that give rise to an oriented growth along the c-axis and a needle-like morphology can be justified. Similarities in crystallographic properties is showed in Table 2.1. Lattice parameters (± 0.003 Å) between enamel, dentin, bone, and HA as reported by (S. Dorozhkin, 2007).

Table 2.1. Crystallographic properties: Lattice parameters (± 0.003 Å).

| Composition, wt% | Enamel | Dentine | Bone | HA |
|-------------------------------|--------|---------|-------|-------|
| <i>a</i> -axis (Å) | 9.441 | 9.421 | 9.410 | 9.430 |
| <i>c</i> -axis (Å) | 6.880 | 6.887 | 6.890 | 6.891 |
| Crystallinity index, (HA=100) | 70-75 | 33-37 | 33-37 | 100 |

The synthetic hydroxyapatite is similar in composition to the mineral component of bone and teeth as shown in the Table 2.2. This similarity makes it the most clinically used as biomaterials for medical and dental applications (Al-Sanabani *et al.*, 2013).

Table 2.2. Chemical and structural comparison of teeth, bone, and hydroxyapatite.

| Composition wt% | Enamel | Dentine | Bone | HA |
|---------------------|--------|---------|------|------|
| Calcium | 36.5 | 35.1 | 34.8 | 39.6 |
| Phosphorus | 17.1 | 16.9 | 15.2 | 18.5 |
| Ca/P ratio | 1.63 | 1.61 | 1.71 | 1.67 |
| Total inorganic (%) | 97 | 70 | 65 | 100 |

| | | | | |
|-------------------|-----|----|----|---|
| Total organic (%) | 1.5 | 20 | 25 | - |
| Water (%) | 1.5 | 10 | 10 | - |

The non-toxic compound and interfacial bonds are able to develop between HA and the living tissues leading to enhance mechanical strength of the overall structures. In the finite element analysis (FE), the analysis approach applied to the mechanical behaviour of this porous model under nano indentation tests has provided better understanding about the influence of pore characteristics (morphology, size and distribution) on mechanical properties of porous HA for biomedical applications (Naderi *et al.*, 2016). Typically, HA also presented poor mechanical properties such as low strength and limited fatigue resistance restrict its application as pure material for the implementation of HA, even though it is widely used for the hard tissue replacement due to their biocompatibility and osteoconductive properties. One way to solve these problem is to apply HA coatings onto biocompatible metal substrates so as to achieved the necessary mechanical strength and bioactive properties at the same time (Lynn and DuQuesnay, 2002, Xiao *et al.*, 2005).

In the HA-based composites, the inadequate mechanical strength of HA ceramics has restricted their application clinically. An appropriate additive may be needed to improve the mechanical characteristics of these HA ceramics. However, flexural strength, strain-to-failure, and fracture toughness values of HA ceramics are significantly less than those of bone, whereas the elastic modulus is much higher. This mechanical mismatch influences the reliability of ceramics when implanted into bone tissue. To improve the mechanical compatibility, a composite approach may be promising. The combination of different materials within a composite structure may lead to a composite material that reveals specific physical, chemical and mechanical properties, particularly resulted from

a synergy principal. Furthermore, in their biological properties, the primarily biocompatibility with living tissue must remain unchanged.

HA possesses low mechanical strength even though it has favourable bioactive and osteoconductive properties that results in rapid bone formation in a host body and strong biological fixation to bone tissues (Al-Sarraf *et al.*, 1997). This has led to an obstacle for the applications in load bearing areas. Thus, the enhancement of the mechanical properties of HA would extend its scope and applications due to the low mechanical strength. In fact, HA is either used as a bioactive coating on implants or reinforced with tough phases such as metal or ceramic phases for biomedical applications. Previous studies have stated that HA have been used successfully in clinical and animal studies for endodontic treatment including pulp capping, repair of mechanical bifurcation perforation, apical barrier formation and repair of periapical defects (Jean *et al.*, 1988, Utneja *et al.*, 2015). The degree of mineralization of reparative dentine obtained with tricalcium phosphate-hydroxyapatite that was quicker and thicker when compared with that produced by calcium hydroxide (Jean *et al.*, 1988).

However, according to a sintering system of HA at high temperatures could affect the decomposition, which starts with dihydroxylation at approximately 900 °C in air and at 850 °C in a water-free-atmosphere. When decomposition occurred, tetra calcium phosphate (TTCP) and tri calcium phosphate (TCP) were produced. The occurrence of TCP consists of β -TCP at <1200 °C and α -TCP at >1200 °C. HA loses many hydroxyl groups above 1300 °C and thus loses significant weight. The strength of HA drastically decreases as temperatures >1350 °C (Arifin *et al.*, 2014, Knowles *et al.*, 1996, Tonsuaadu *et al.*, 2011).

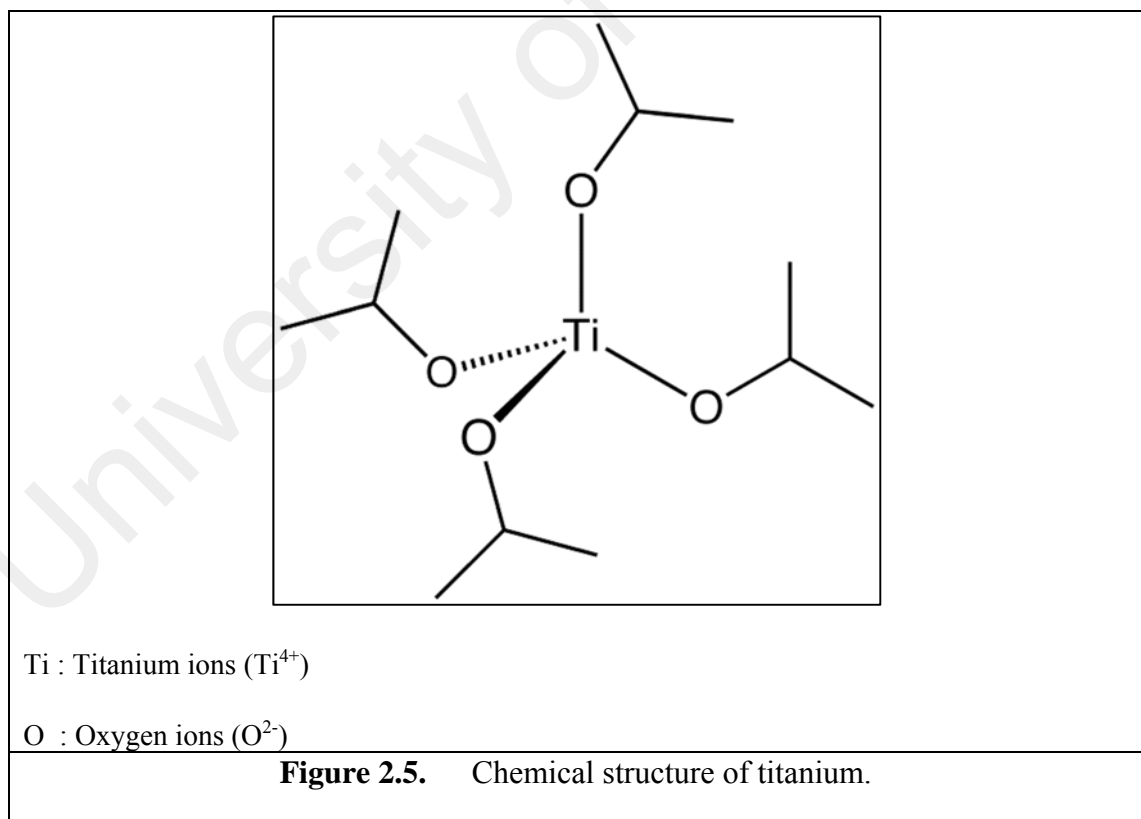
2.4.2 Titanium

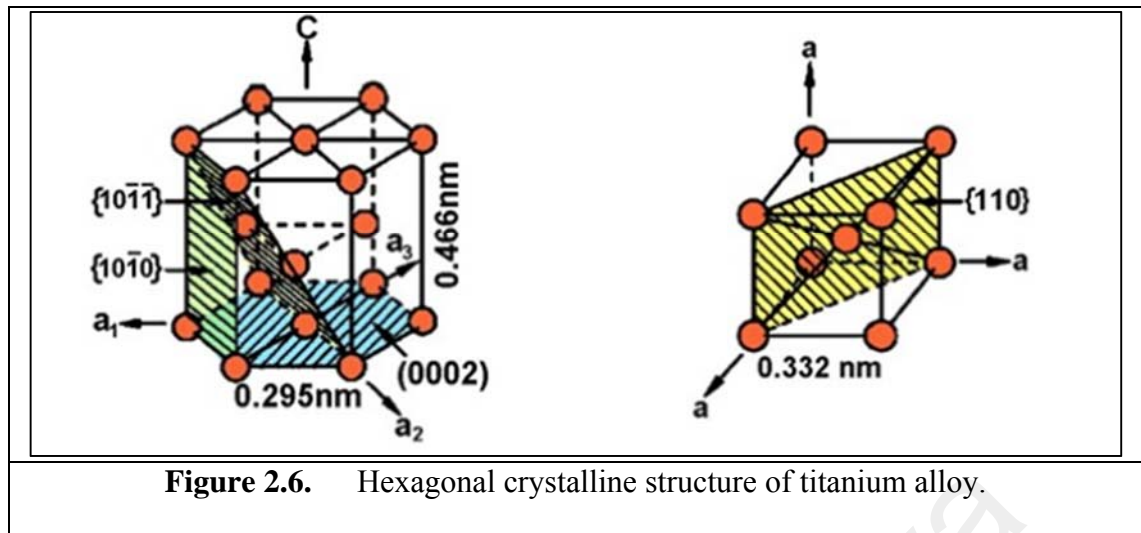
For enhancement of the mechanical properties, titanium (Ti) has become a popular metallic biomaterial because of its properties for many biomechanical applications including dentistry since 1960's. On the other hand, the use of Ti as an implant material has become an integral part of dental therapy. Pure Ti and Ti-6Al-4V type alloys are also the main implant materials in the dental field (Niinomi, 1998). According to a previous study, Ti-6Al-4V indicating that alloy contains 6% aluminium and 4% vanadium that lead to improved mechanical strength and fracture resistance (Elias *et al.*, 2008). The improvement in the bioactivity will greatly enhance the performance of the Ti implants (H. Ye *et al.*, 2009). In fact, the biomolecule absorption is reflected by an increased cell adhesion and subsequent osseointegration (Bruschi *et al.*, 2015).

With the compliance of good biocompatibility and low density coupled with good balance of mechanical properties and corrosion resistance make this material different from others. However, Ti is a bioinert material and cannot promote tissue bonding to the implants (Liu *et al.*, 2004). Thus, the interface between Ti and host bone is a simple interlocking bonding which can lead to the loosening of the implant and the eventual failure of the implantation (Balbinotti *et al.*, 2011). The response to the particular Ti of its advantages can also lead to the low module of elasticity, close to the bone/teeth. Ti alloys can be divided into α -, ($\alpha + \beta$)-, and β -type alloys. β -type alloys have the lowest Young's modulus, which is closest to the Young's modulus of bone (10-30 GPa) (Arifin *et al.*, 2014). With the density of Ti, 4.5 g/cm³ and a melting point of 1668 °C, Ti becomes reactive with other materials (Traini *et al.*, 2008). Ti alloy has a tensile strength of approximately 1400 MPa at room temperature. Therefore, the stiffness of Ti is generally not well adapted to bone or teeth and this can lead to stress shielding of the residual

bone/teeth, which may result in detrimental resorptive bone remodeling (Traini *et al.*, 2008).

Titanium (Ti) is chosen as a metallic implant due to its well-known superior mechanical properties that make them withstand load bearing applications (Morks *et al.*, 2008). A grain of Ti is formed by the aggregate of a group of similar crystals of a given metal (or alloy). Titanium which has a hexagonal close-packed (hcp) crystal structure is referred to as 'alpha' phase. Another transformation into body-centered cubic (bcc) crystal structure, called 'beta' phase, at 888°C (1621 °F). Both categories denote the general type of microstructure after processing. This microstructure refers to the phases and grain structure present in a metallic component which affect the grain shape and size behaviour when crystal structure changes (Leyens and Peters, 2003).





HA-Ti FGM can make a promising material for tissue implantation, orthopedic, and dental applications because of its outstanding biocompatibility and bioactivity. There are fabrication methods used such as Cold Isostatic Press (CIP), Spark Plasma Sintering (SPS), Hot Pressing, and Powder Metallurgy (PM). The synthesis of HA-Ti as a FGM dental implant using cold isostatic press (CIP) and sintered by high frequency induction heating can satisfy both its mechanical and biocompatible properties (Watari *et al.*, 1997).

There is also a sintered electric furnace heating (EF) and SPS method for sintering. In the EF sintering, powders were packed into the thermal contractive tube after heat treatment of a tube at 60 °C, which was then compressed by CIP at 800-1000 MPa and sintering in a vacuum at 1300 °C densified the implants of the miniature cylindrical shape. In the high frequency induction heating, they packed powders into the thermo contractive tube or silicon rubber impression mold with the shape of a dental implant. After CIP, the packing were sintered at above 1300 °C in argon gas atmosphere (Watari *et al.*, 2004).

In the high frequency induction heating, they packed powders into the thermo-contractive tube or silicon rubber impression mold with the shape of a dental implant. For SPS process, the mixed powders of Ti hydrate and HA were put into a graphite mold with the gradient composition ranging from 100% Ti to pure HA in the height direction and

sintered at 850 °C at a pressure of 40 or 80 MPa. (Watari *et al.*, 1997) reported that Ti with 100 wt.% HA FGM decomposition in the sintering process is significant. Internal stress also arises from the difference of thermal expansion coefficient and shrinkage at the interface from one region to other.

Moreover, they lowered the sintering temperature by using SPS to avoid auto destruction. Much improvement occurs in sintering by SPS compared with the conventional CIP and furnace sintering methods. Fracture of the FGM occurs near the weakest region or its neighbour. In the three-point flexural test of HA-Ti FGM prepared with SPS at a pressure of 40 MPa, fracture occurred deviated from the center in the HA rich side, which is weaker. In the FGM prepared with 80 MPa, fracture occurs inside the single layer in the center. The flexural strength increased to 36 MPa and the compressive strength was 88 MPa, respectively.

2.5 Coating Titanium Particles with a Silica

Arising from the continuous generation make the improvement in the bonding between the implant and growing bone using HA surface layers which has been demonstrated in many studies (Borum and Wilson, 2003). When HA is added to these surface layers, the species for promotion of bone growth in some forms of silicate or silica species has been shown. Silicon-rich materials, such as bio glasses and glass ceramics that contain high concentrations of silica could successfully used as biomaterials to promote bone growth (Sadjadi *et al.*, 2011). The thin silica layers prior to mixing with HA could prevent the undesired metallic-ceramic reactions at increased temperatures when coated with the Ti particles.

Silica (SiO_2) act as one particular approach to address this issue in the incorporation of low-melting-point biocompatible additives as sintering aids to the initial

components. Therefore, by removing the fragile compounds, the resulting composite may provide improved mechanical strength for load-bearing application (Wakily *et al.*, 2015). The benefits of using silica has been elaborated in a simple understanding in related to increasing the properties of coated silica with Ti and HA interfaces. Silica, which is a stable oxide of silicon (SiO_2), is a bioactive material with high corrosion resistance. Carlisle (1970) established a biological basis for the role of silica in bone formation. Silica is thought to perform a specific metabolic function that partakes in cellular development and gene expression (Hing *et al.*, 2006).

Secondly, the existence of chemical functions in the silica structure could enhance the precipitation of an apatite layer on the surface of bioactive materials. SiO_2 inhibit bacteria adherence to oral biofilms and proliferation of bacteria (Besinis *et al.*, 2014). The silica particles can improve the strength of HA coatings by particle-mediated reinforcement, leading to crack deflection or crack arrest. Therefore, silica is believed to play a critical role in bioactive materials by acting as a cross-linking agent in connective tissue, providing sufficient integration with the bone structure (Morks *et al.*, 2008, Sadjadi *et al.*, 2011).

It is important that the silica coating on the titanium be dense rather than porous and be present as a film or skin around the individual Ti particles. When silica-coated with Ti particles are synthesized, it is allowing the minimization of unfavorable inter-phase reactions in the HA-Ti composites. The amount of silica present as free silica fragments or gel should be a minimum. Under electron microscope examination at a high degree of magnification, the nature of the coating on the titanium particles can be readily seen, because the density of titanium is roughly about twice that of silica and the electron beam penetrates the silica more readily than the titanium, thus giving a sharp contrast in the density of the image on the electron micrographs.

In contrast, in electron micrographs of titanium particles, which silica has been precipitated indiscriminately by conventional methods, the silica is present as a voluminous mass of extremely fine particles (Werner, 1969). It is expected that with the incorporation of silica-coated titanium (STP) resulted complete removal of CaTiO_3 and Ti_xP_y phases from the sintered composites. By the addition of silica, the secondary calcium phosphates produced from HA decomposition remain stable at sintering temperatures, resulting in less physical stress during the cooling process. The present study focuses on the surface of titania-coated silica particles which formed as textured.

The titania-coated silica particles are spherical, monodisperse, and not agglomerated. The morphology of titania-coated silica particles from synthesized titania-coated silica was reported (Hanprasopwattana *et al.*, 1997). While for silica modified HA include the enhancement in colloidal stability, resistance to dissolution in acid environments, potential for enhance interfacial bond formation when used with silane coupling agents in nanocomposite development, and enhanced bioactivity due to the established role of silica in bone formation (Borum and Wilson, 2003).

Chapter 3

Materials and Methods

Fabrication of the functionally graded structures using silica-coated titanium (STP) and hydroxyapatite (HA) via the powder metallurgy (PM) approach consists of the selection and optimization of the metal/ceramic combination, step-wise or continuous stacking of powder premixes according to the pre-designed compositional profile, hydraulic pressing, cold isostatic compaction, and sintering of the pressed powder. The focus of this study is to minimize the aggressive reactions of titanium (Ti) with the HA ceramic phase in different layers of the FGM structure. For this aim, the Ti particles are coated by a thin silica (SiO_2) layer which acts as a protective film between the Ti and HA phases. The protocol employed for synthesis of silica-coated titanium (STP) is being discussed in detail.

The morphological, chemical, and mechanical properties of the FGM layers were also characterized by various techniques to predict their performance in the FGM structure. The obtained results were then fed back to the design process to optimize the FGM properties.

3.1 Preparation of HA and Ti Powders

As mentioned before, the FGM layers were mainly fabricated from commercial Ti and HA powders as the metallic and ceramic components, respectively. The general information of these two materials is given in Table 3.1. The HA powder used in this study was obtained from Sigma Aldrich, while the Ti powder was purchased from R&M Chemicals. The materials needed for synthesis of silica including tetraethylorthosilicate (TEOS) and ammonia (25% v/v) were also purchased from Sigma-Aldrich (Table 3.2).

Table 3.1. Physical and chemical properties of green powders used in the study.

| Properties | Ti | HA |
|---------------------|-----------------------|--|
| Formula | Ti | Ca ₅ (PO ₄) ₃ (OH) |
| Physical state | Powder | Powder |
| Particle size | <45 µm | ~ 5 µm |
| Purity | ~ 99% | ≥90% |
| Density | 4.510 | - |
| Molecular weight | 47.90 | 502.31 |
| Boiling point | 3287 °C | n/a |
| Melting point | 1660 °C | 1100 °C |
| Solubility in water | insoluble | solvent |
| Manufacturer | R&M Chemicals | Sigma-Aldrich |
| City / Country | Essex, United Kingdom | St. Louis, USA |
| Batch No. | PBSV100712 | MKBK2210V |

Table 3.2. Specification of solutions in the study.

| Solution | TEOS | Ammonia |
|---------------------|--|--------------------|
| Formula | C ₈ H ₂₀ O ₄ Si | NH ₄ OH |
| Solubility in water | insoluble | insoluble |
| Manufacturer | Sigma-Aldrich | Sigma-Aldrich |
| City / Country | Hohenbrunn, Germany | St. Louis, USA |
| Batch No. | STBC0106V | A0333193 |

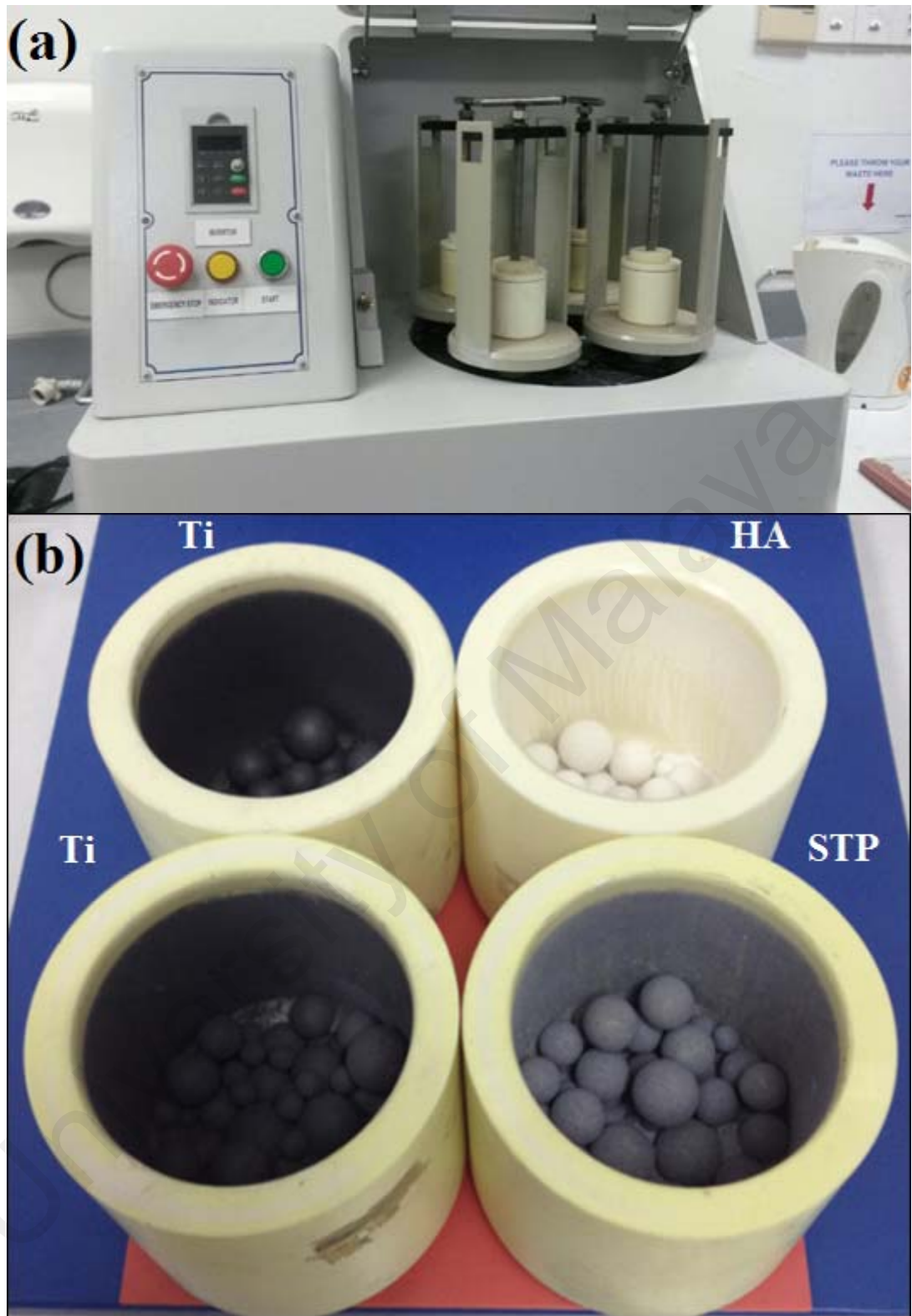


Figure 3.1. (a) The ball milling machine, and (b) the cups and balls used for milling the HA and Ti powders.



Figure 3.2. The HA and Ti powders after grinding in the ball mill machine.

According to the manufacturers' information, the average particle sizes of HA and Ti powders were 5 μm and 45 μm , respectively. However, our analyses showed that the particle sizes of the obtained powders were not well distributed and contain large particles which may negatively affect the mechanical properties of the FGM structure. Therefore, the particles were firstly milled to achieve a more uniform particle size distribution. For this aim, a planetary ball mill machine (Retch Germany, 200 rpm) with ceramic cups (Figure 3.1) was used. The HA and Ti powders weighing 10 grams were milled separately using zirconia ceramic balls of 1/4 inch in diameter for 1 hour to promote homogeneity of the powders and decrease the particle size. The blending process was carried out at 200 rpm with reverse action for an hour. The powders were then dried in an oven at 110°C for at least 12 hours to produce a mixture with no moisture (Figure 3.2).

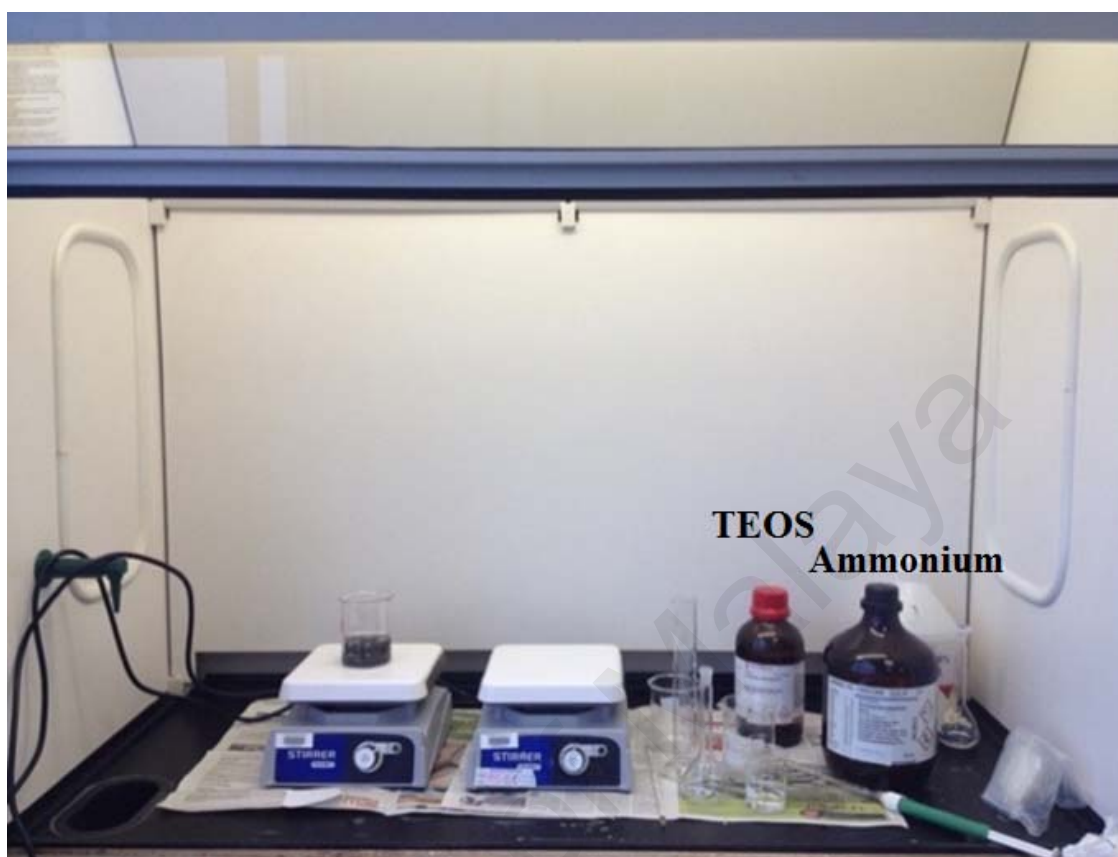


Figure 3.3. Experimental setup for synthesizing silica-coated titanium (STP).

3.2 Synthesis of Silica-coated Titanium (STP) Powder

The experimental setup for synthesis of STP powder is shown in Figure 3.3. In this approach, the Ti particles are coated by thin silica layers prior to mixing with HA to prevent the undesired metallic-ceramic reactions at increased temperatures. Thus, by removing the fragile compounds, the resulting composite may provide improved mechanical strength for load-bearing application. For synthesis of STP powder, 1 gram of pure blended titanium powder (commercial $\sim 45\ \mu\text{m}$) was stirred in 100 ml of ethanol-water solution (10:1) using a standard magnetic stirrer, followed by injecting ammonia solution to achieve a pH of 12.5. Addition of ethanol could result in accelerated hydrolysis reaction of TEOS and also lead to the homogenization of the solution. Then 4.67 ml of

TEOS was added and the mixture was stirred for 4 hours to initiate the silica formation. A mixture transformation from black colour to grey confirmed formation of SiO_2 (Figure 3.4). After stirring, the mixture was aged for 24 hours to allow precipitation of the particles. The solution containing unattached SiO_2 was firstly sucked by a pipette (Figure 3.5). The remaining precipitate was then rinsed with deionized water and centrifuged to completely remove unattached polysiloxane oligomers. The obtained STP particles were then dried at 60°C for 6 hours.



Figure 3.4. Stirring of titanium powder at 800 rotation per minute (rpm) for 4 hours.



Figure 3.5. Initial suction of the unattached silica by a pipette.

3.3 Powder Processing Technique

3.3.1 Drying

HA, Ti and STP powders were dried in an oven (Figure 3.6) at 100 °C for at least 6 hours to produce a dry mixture with no moisture. This procedure prevents the particles from being sticky, and thus minimizing the formation of agglomerates of the particle during mixing.



Figure 3.6. The oven used to dry HA, Ti and STP powders.

3.3.2 Milling of the STP Powder

The obtained STP powder was again milled in the planetary ball mill machine in order to achieve suitable particle distributions and reduce the possible particles aggregation due to formation of the silica layers on the Ti particles.

Milling and mixing are the crucial steps in specimens' preparation. An effective mixing and milling process will result in lower amount of agglomerates and a uniform composition in the mixture. For objective 1, the HA and Ti powders with equal weight ratios were milled using planetary ball mill with zirconia balls to ensure maximum

dispersion of particles. The mixed powders of HA-STP were checked for every 1 hour to avoid the powders sticking onto the wall of the bowl because of the high adhesive properties of HA in comparison with STP in the mixing powders.

The obtained powder (Figure 3.7) was then compacted under 450 MPa, calcinated at 850 °C for 2 hours and sintered at 1100 °C for 1 hour under argon atmosphere. Similar protocol was applied to produce composites with HA-Ti weight ratios of 1.0 (HA-Ti) and 0.33 (Ti3-HA) as references to investigate the influence of silica on the chemical and mechanical properties of HA-STP composites.

The cleaning of the ball mill equipment (bowl and balls) consists of four steps:

- a) Hydrochloric/hydrophosphoric acid ($\text{HCl}/\text{H}_3\text{PO}_4$) solution
- b) Mineral water cleaning
- c) Soft cloths
- d) Ethanol

Treatment with the $\text{HCl}/\text{H}_3\text{PO}_4$ solution was done for 20 minutes which was followed by washing with mineral water and drying with soft cloths. Finally, ethanol was used for washing.

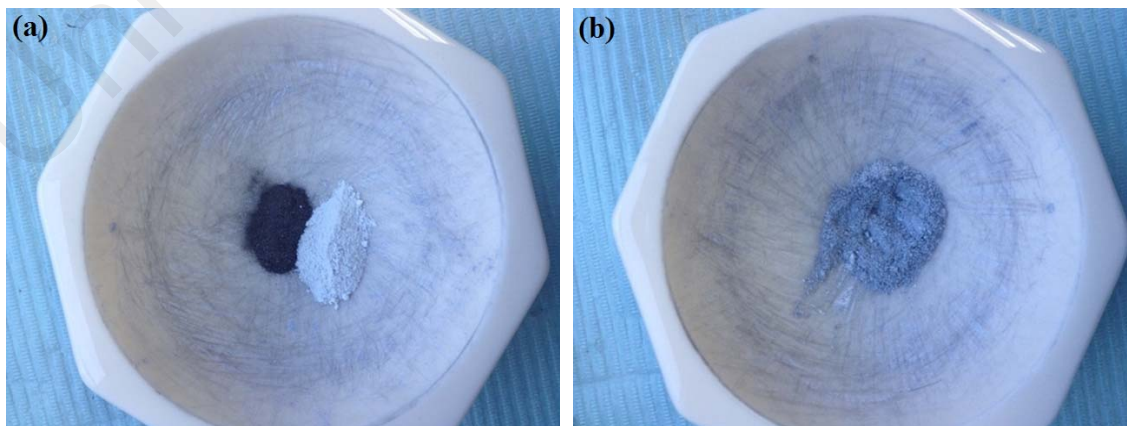


Figure 3.7. (a) HA and STP powders before mixing and (b) homogeneous mixing of HA-STP using ceramic mortar.

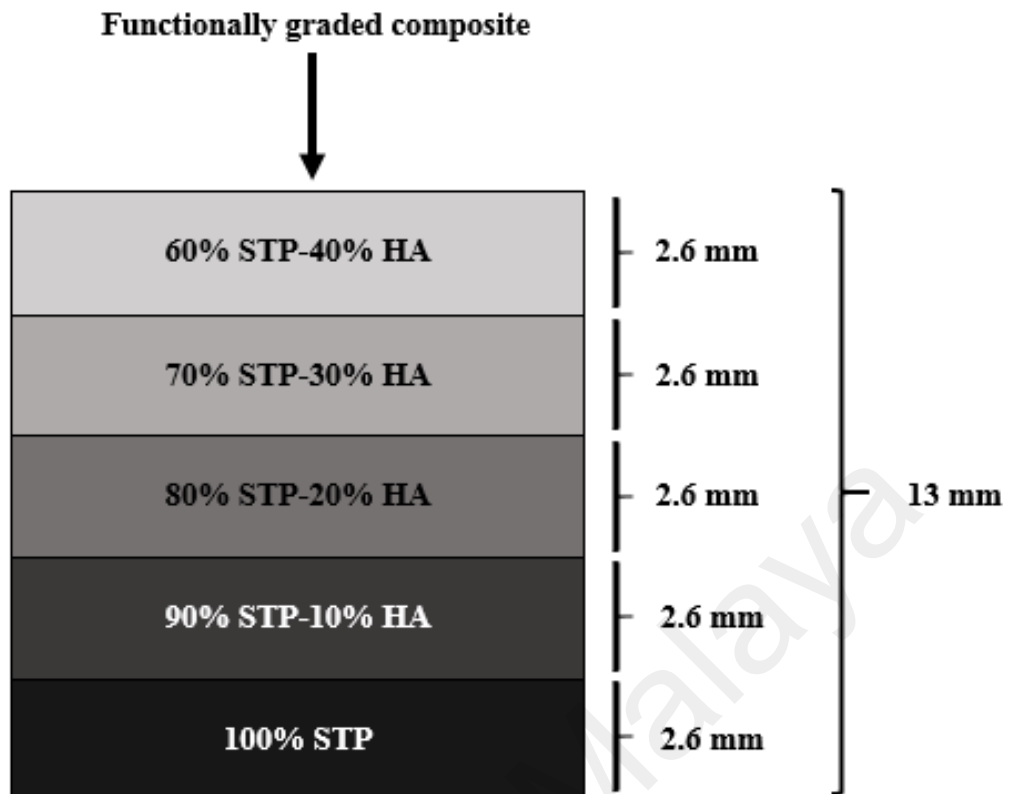


Figure 3.8. Schematic illustration of multilayered and composition of each layer HA-STP of the fabricated specimens.

3.4 FGM Fabrication

Based on the second objective, to fabricate a new type of FGM using HA and STP, five STP-rich layers with different STP/HA weight ratios including 10/0, 9/1, 8/2, 7/3, and 6/4 were prepared and each layer ingredients were again milled for 5 hours to obtain homogeneous mixture in each layer. The effective mixing and milling process will result in lower amount of agglomerates and a uniform composition in the mixture. The quantities of powders were taken such that thickness of each individual layer was approximately 2.6 mm and thus, the thickness of final FGM obtained was ~13 mm with 8 mm diameter of the compacted specimen due to its common used devices in the clinical studies. Figure 3.8 portrays a schematic of the FGM structure comprised of five best layers with different compositions to produce a gradually stable FGM composites.

3.4.1 Compaction using Uniaxial Hydraulic Press

In this study, instead of direct pouring the green powder inside the mould, a flexible plastic pipe with external diameter equal to the internal diameter of the stainless steel mould was used (Figure 3.9 (a)) to facilitate sample removal from the mould. The pipe was cut with similar height to the mould, placed inside the mould hole, and the powder was poured in the tube. The internal surface of the stainless steel mould was also lubricated using zinc stearate (Figure 3.9 (b)) to facilitate the tube removal after compaction. Preliminary investigations also showed that insertion of the 10/0 layer first could facilitate removal of the specimen after compaction without causing any damage to the specimen. After each layer had been placed, the plunger was inserted to flatten each layer using a gentle pressure (Figure 3.10). The powder was then compacted in two directions under 450 MPa by using a uniaxial hydraulic pressing machine (Figure 3.11) for 10 minutes forming a rod shaped specimens. After ejecting from the mould, the tube was cut using a cutter to remove the pressed specimens.



Figure 3.9. (a) The flexible plastic tube, and (b) the lubricant materials.

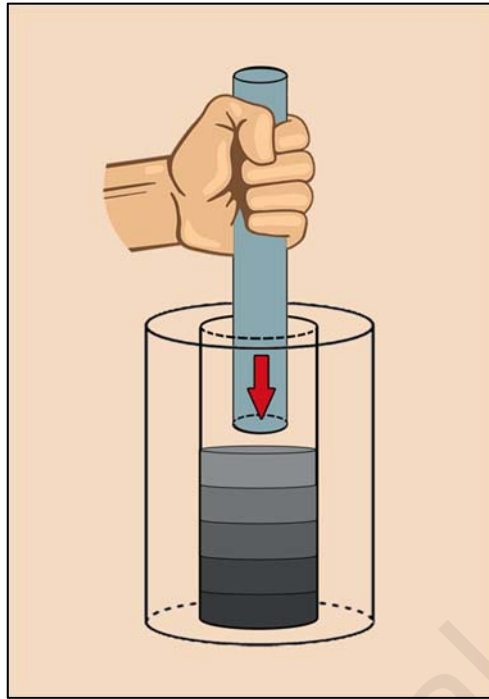


Figure 3.10. Schematic of the method used to flatten the FGM layers with a gentle pressure using plunger.



Figure 3.11. Compaction of green FGM specimen by hydraulic press machine.

3.4.1.1 Cold Isostatic Press

Since pressing of the specimens by hydraulic press was not sufficient, cold isostatic pressing (CIP) was used at 2500 MPa to perform samples compaction from every direction (Figure 3.12 (a)). To maintain the outer shape of the specimen during pressing and avoid contact to the pressing oil, the specimens were placed inside a rubber glove before placing into the fluid container (Figure 3.12 (b)). Therefore, the pressure transmitting fluid could easily apply the compacting pressure on the rubber glove.





Figure 3.12. (a) Cold isostatic press machine and (b) the rubber glove used to protect the specimens from contamination by the CIP oil.

3.4.2 Sintering

The final mixed heterogeneous FGM samples were sintered in a normal furnace (Figure 3.13 (a)) with air atmosphere at 1100°C for 3 hours with heating rate of 5 °C/min (Figure 3.13 (b)). The temperature of the furnace was set and monitored using the digital program controller. This stage allows densification of the FGM specimens. Finally, the temperature was decreased gradually from 1100 °C to 50 °C by keeping the specimens in the furnace overnight. A typical image of a sintered FGM is also shown in Figure 3.14.

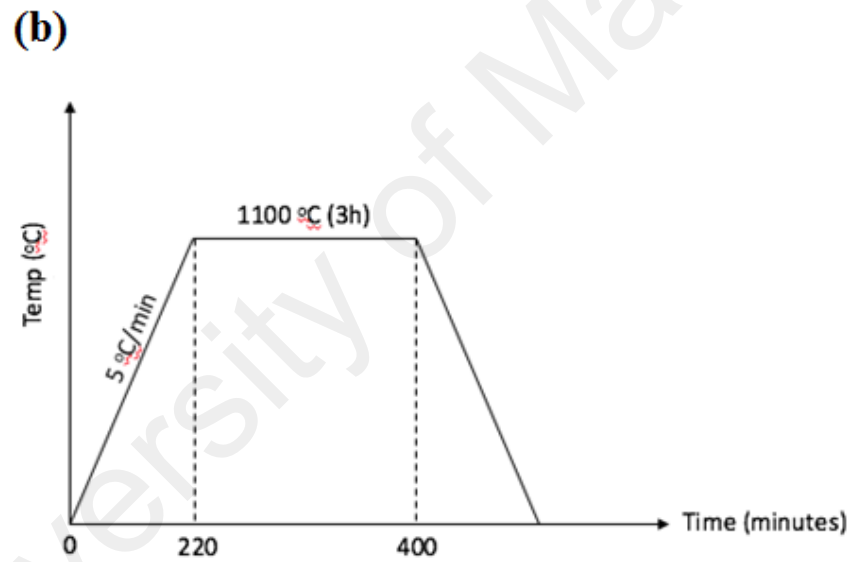
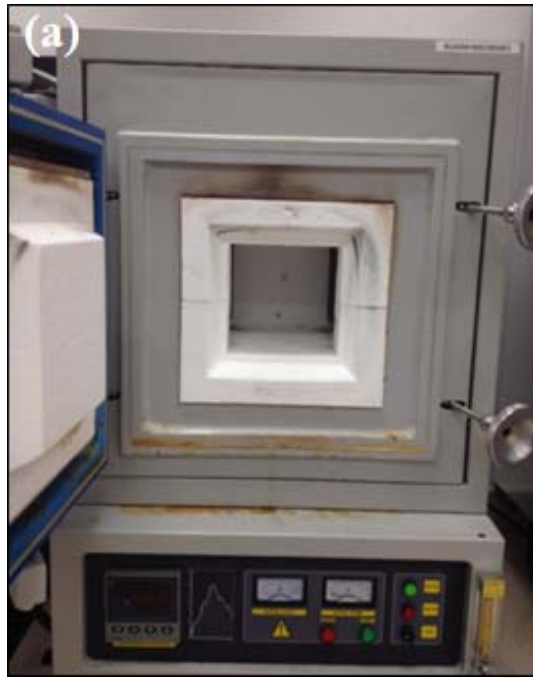


Figure 3.13. (a) The sintering furnace, and (b) the sintering cycle used in this study.



Figure 3.14. A typical FGM specimen after sintering.

3.5 Characterization Techniques

3.5.1 Morphological Properties

The structural morphology of the STP powder was evaluated under 3D-surface texture Analyser (Alicona, Infinite Focus, USA) in order to confirm formation of a silica layer around Ti particles. The scanning electron microscopy (SEM; Quanta 250 FEG, FEI Inc., USA) was also employed to investigate the morphological properties of different FGM layers.

3.5.2 Chemical Properties

X-ray diffractometry (XRD: Philips PW1840) (Figure 3.15) was employed to observe the possible phase changes of HA and Ti during the sintering procedure. The measurements were carried out using a Siemens D5000 X-ray diffractometer and using Cu K X-ray source radiation ($\lambda = 1.5418\text{\AA}$) and scan rate of $0.02^\circ/\text{s}$. The specimens were mounted onto holders using a viscous adhesive and adjusted to the correct height with a glass slide. In order to obtain the graded compositional profile, the specimens were cut using diamond blade into consecutive slices of 2 mm thick at each layer representing the different composition. The peaks obtained were then compared to the standard reference JCPDS-ICCD (Joint committee of powder diffraction Standard-International Centre for Diffraction Data) files to assess the phases in specimens. The obtained results of the XRD analyses were further confirmed using Fourier transform infrared spectroscopy (FT-IR: Thermoscientific, Nicolet 6700). The energy dispersive X-ray spectroscopy (EDX: FEI Quanta 250) was carried out on the top surfaces of FGM to provide complimentary information about the elemental composition of the composites.



Figure 3.15. The X-ray diffraction machine used in this study.

3.5.3 Physical Properties

The bulk densities of different layers of FGM structure were determined by water immersion techniques on the Archimedes principle using an electronic densitometer (SD-200L, Japan). The specimen was inserted into the upper cup of the densitometer and the weight was recorded in the balance, following which the specimen was removed and then placed into the lower cup which was also filled with water. After that, again the weight was recorded. Based on the Archimedes' principle, the difference between the two recorded values is equal to the weight of the water displaced by the specimen. The density was then calculated according to the following equation:

$$\rho = \frac{W_a}{W_a - W_w} \quad (3.1)$$

Where W_a and W_w respectively represent the weight in air and weight in water. The measurements were repeated at least four times to reduce any errors and to produce a repeatability of the measurement.

The volumetric expansion (or shrinkage) after sintering was also calculated by the following equation:

$$\text{Volumetric Expansion}(\%) = \frac{V_s - V_g}{V_g} \times 100 \quad (3.2)$$

Where V_g and V_s are the specimen volume before and after sintering, respectively.

3.5.4 Mechanical Properties

Mechanical property evaluation of HA-STP and different FGM layers was determined by testing the hardness (HV) using Vickers indentation machine (Shimadzu, Japan) as shown in Figure 3.16 at a load of 100g. This technique is ideal for both sintered disc specimens representing layer of the FGM and the FGM specimens. The indenter is pyramidal in geometry with known angles on each side. Using a known load, the microhardness was calculated automatically by measuring the length of the diagonals of the indent of the surface of the material where the smaller the indentations correspond to the harder materials. At least five indentations were performed for each layer to calculate micro-hardness values of layers by fixed load from indenter.



Figure 3.16. Microhardness testing machine using Vickers hardness method.

Chapter 4

Results

4.1 HA-STP Single Layer

4.1.1 STP Microstructure

The microscopic images of the Ti and STP powders are illustrated in Figure 4.1 (a) and (b), respectively. The black and shiny phases in Figure 4.1 (a) indicated the Ti particles, while the second image shows a decreased metallic luminescence, possibly due to the formation of silica protective layers around the Ti particles.

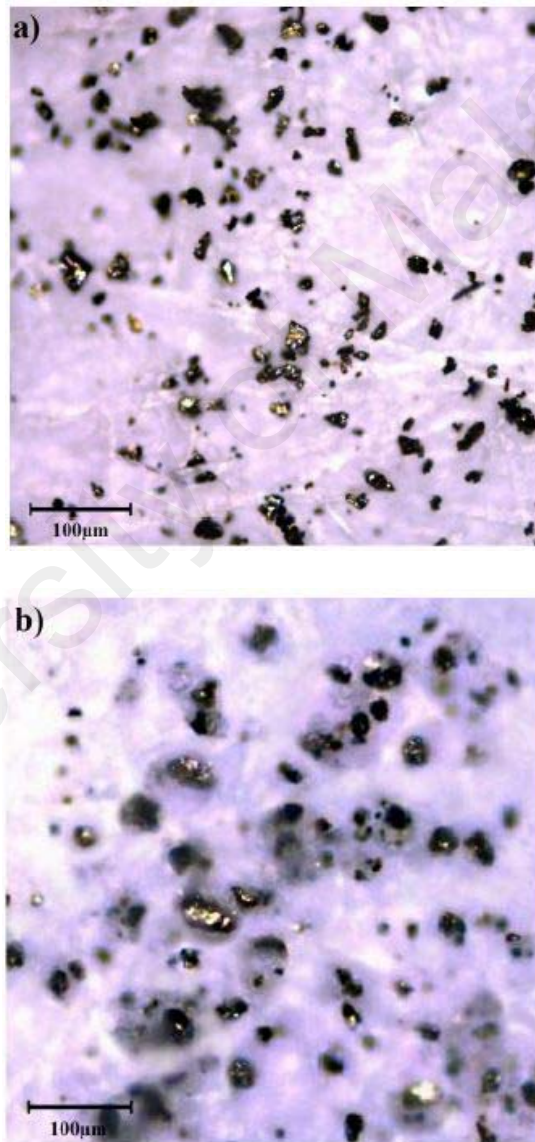


Figure 4.1. The microscopic images of (a) Ti, and (b) STP.

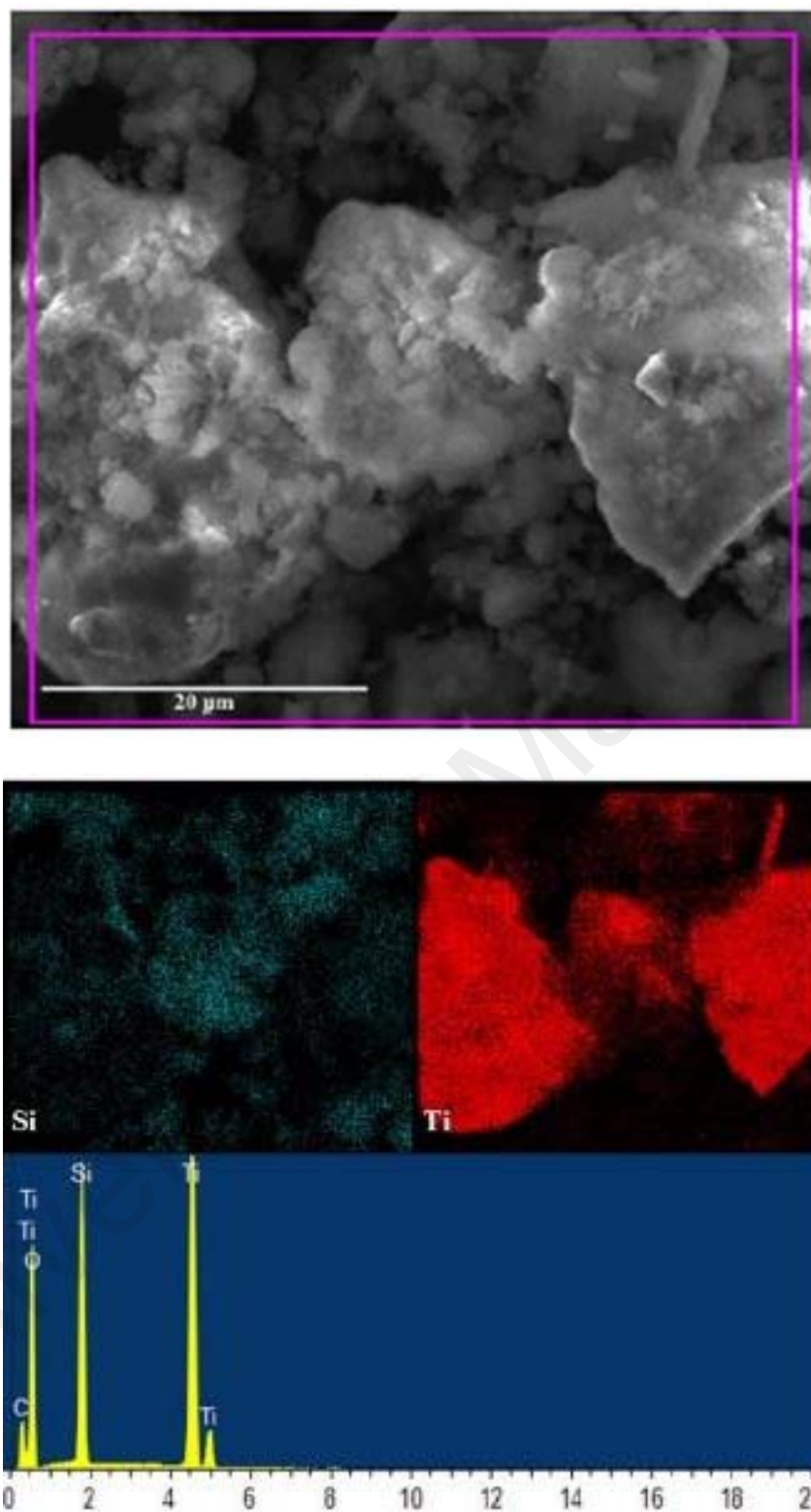


Figure 4.2. EDX analysis of the STP powder.

Energy-dispersive X-ray spectroscopy (EDX) analysis is used as an analytical technique for the elemental analysis or chemical characterization of a sample. The

obtained result of EDX, map distribution, and the intensity peaks of Ti and Si elements in the STP powder are also shown in Figure 4.2. According to figure 4.1, the surfaces of coarse Ti particles are covered with an almost uniform silica layer composed of fine particles. Formation of this inert ceramic layer could possibly result in reduced contact between the Ti and HA phases and thus, decrease formation of the undesired brittle phases in the sintered products, which drastically affect their mechanical behavior.

4.1.2 Chemical Stability of the HA-STP Single Layer

In Figure 4.3 the XRD patterns of Ti, STP, sintered HA-Ti, and sintered HA-STP specimens are shown. Comparison of the XRD patterns of Ti and STP powders indicated the stability of titanium in the basic environment required for preparation of SiO₂ coating. In the XRD pattern of the sintered HA-Ti composite, the HA and Ti peaks completely disappeared and Ti_xP_y (mostly Ti₅P₃) and TiCaO₃ were the dominant phases. This is clearly shown that undesired reaction between Ti and HA powders in the sintered HA-STP was prevented, causing complete removal of CaTiO₃ and Ti_xP_y.

However, the presence of SiO₂ could not fully protect Ti and HA against oxidation and decomposition to Ca_xP_y, respectively. Due to the similarity of the diffraction peaks of different Ca_xP_y formulations (e.g. HA, oxyapatites, TTCP, α -TCP, β -TCP) and overshadowing their peaks by strong peaks of Ti₂O₃, it was difficult to accurately determine the Ca_xP_y types produced in the composite. When SiO₂ is introduced, the most observed compound obtained was the formation of calcium silicate (mostly CaSiO₃). On the other hand, this compound may exhibit less negative impact on the mechanical properties compared to calcium titanate and titanium phosphides. According to the previous studies, calcium silicate may even show reinforcing influence on the HA matrix (Kaewsichan *et al.*, 2011).

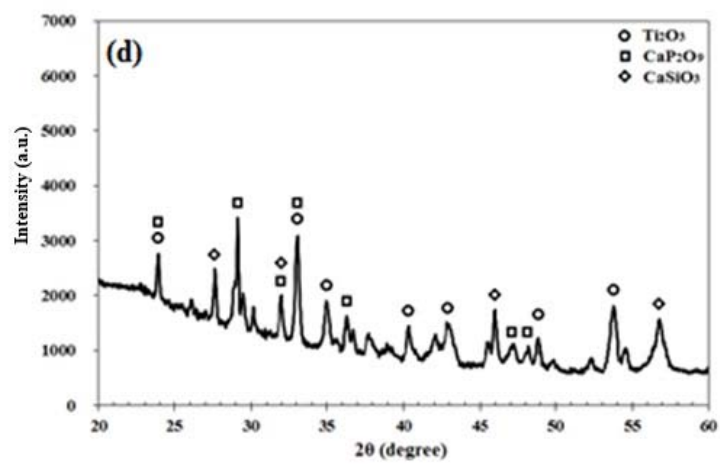
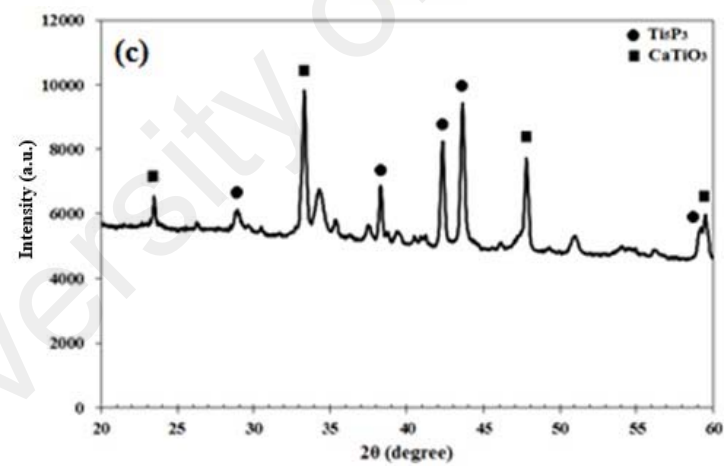
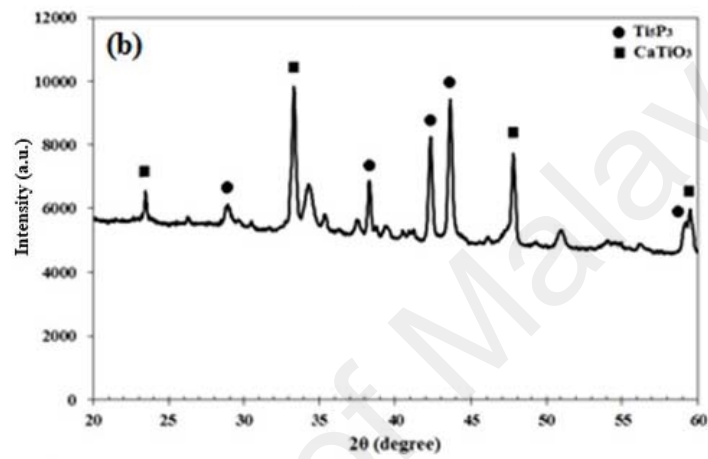
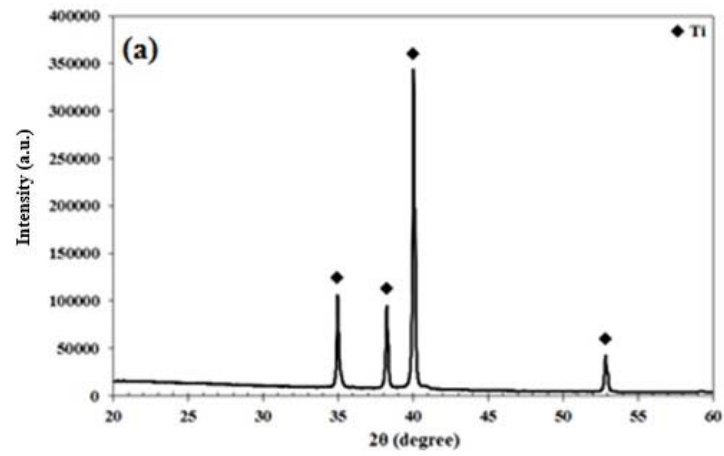


Figure 4.3. The XRD analysis of (a) titanium, (b) silica-coated titanium (STP), (c) sintered HA-Ti, and (d) sintered HA-STP.

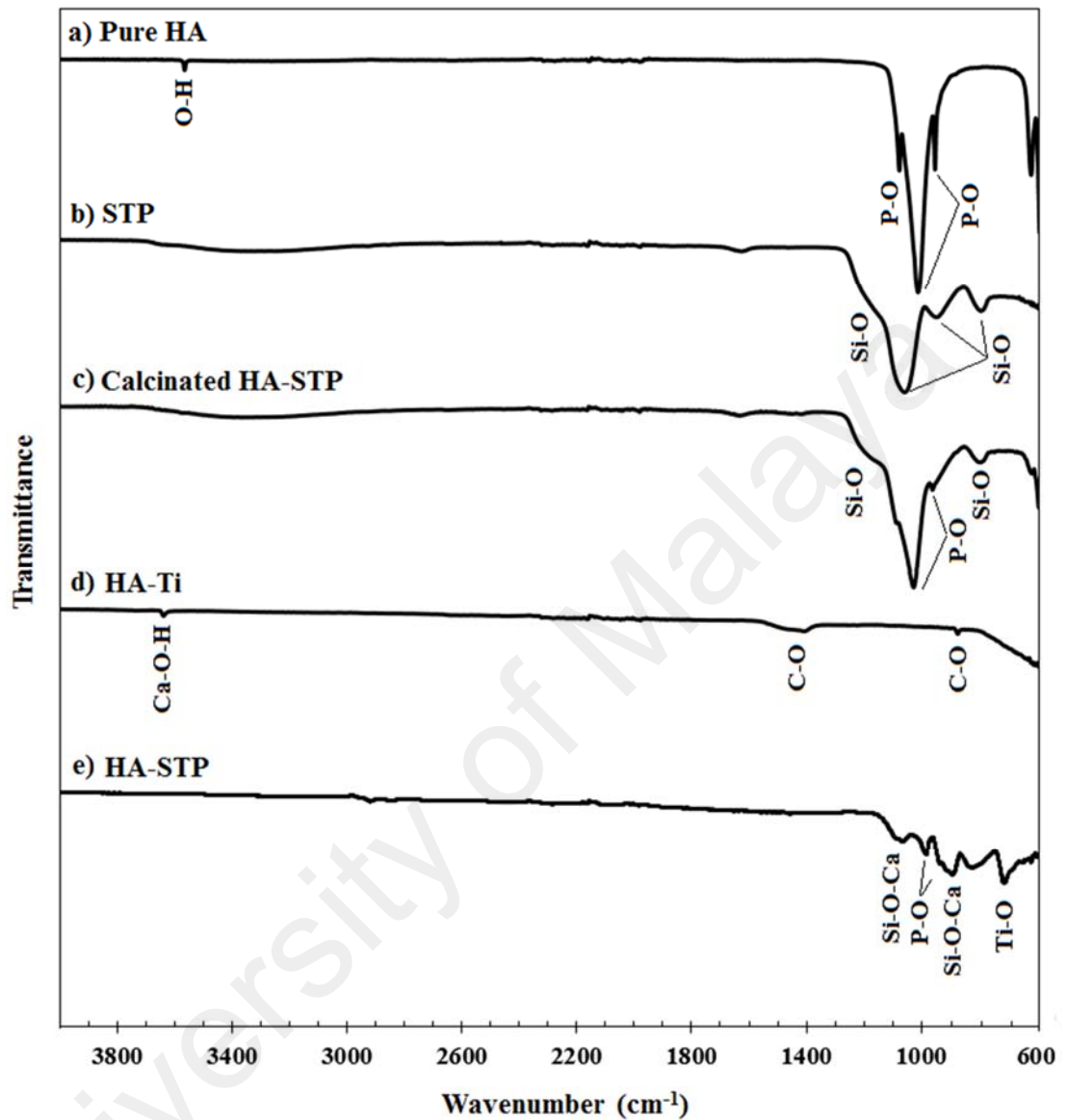


Figure 4.4. The FT-IR spectra of (a) hydroxyapatite (HA), (b) silica-coated titanium (STP), (c) calcinated HA-STP, (d) sintered HA-Ti, and (e) sintered HA-STP.

Figure 4.4 shows the FTIR spectra of the pure HA, pure silica, calcinated HA-STP, sintered HA-Ti, and sintered HA-STP composites. In pure HA, strong peaks observed at 963 cm^{-1} , 1021 cm^{-1} , and 1087 cm^{-1} represented the phosphate (PO_4^{3-}) band, while the weak peak at 3571 cm^{-1} showed the hydroxyl (OH^-) group which is the characteristic band

of the HA structure. In the FT-IR spectrum of the STPs, all the absorption peaks represented the Si-O band. For the calcinated HA-STP, the silane and phosphate peaks were clearly observed. However, due to a low SiO₂/HA ratio, the silane vibration at 1058 cm⁻¹ was overlapped by the phosphate principal peaks.

The FT-IR spectrum of the sintered HA-Ti indicated the elimination of phosphate peaks due to the complete removal of HA during the sintering process. This spectrum was similar to that of pure CaO (Ye *et al.*, 2009) where the peaks at 873 cm⁻¹ and 1400-1600 cm⁻¹ corresponded to the C-O band, while the short peak at 3634 cm⁻¹ represented the Ca-O-H vibration. The carbonate band showed the formation of CaCO₃ to the integration of CaO with CO₂ absorbed during handling and sample preparation (Ye *et al.*, 2009). Elimination of PO₄³⁻ bands demonstrated the complete decomposition of Ca_xP_y phases to an amorphous phase and CaO which further resulted in formation of CaTiO₃ and CaCO₃.

In the HA-STP composite, the phosphate peaks at 940 cm⁻¹ and 970 cm⁻¹ were clearly observed, demonstrating the presence of Ca_xP_y phases. However, the phosphate peaks were different from those of pure HA or oxyapatite (dehydroxylated HA) and fitted with those of β-TCP (Meejoo *et al.*, 2006). The sharp peak at 710 cm⁻¹ also represented the Ti-O band, while the broad peaks at 820 cm⁻¹ and 1600 cm⁻¹ were respectively, attributed to the Si-O band of amorphous silica and Si-O-Ca vibration, indicating the formation of calcium silicate. Therefore, although the HA decomposition was observed in the HA-STP composites, the addition of silica shell around Ti particles inhibited the decomposition of secondary calcium phosphate to CaO.

As results showed the existence of decomposition of hydroxyapatite and oxidation of titanium during the sintering process at 1100 °C, however, the undesired interactions between hydroxyapatite and titanium components were minimized, causing complete

removal of calcium titanate and titanium phosphides as well as formation of stable calcium phosphates in the sintered composite.

4.1.3 Vickers' Hardness of the HA-STP Single Layer

The comparison between Vickers' hardness of the HA-STP composite with those of pure Ti, HA-Ti, and Ti3-HA is provided in the histogram bar graph in the Figure 4.5. The mechanical stability of HA-Ti composite was not sufficient for hardness measurement and thus, the hardness data could not be reported. The low hardness of HA-Ti samples was attributed to the presence of brittle phases (TiCaO_3 and Ti_xP_y) which require temperatures higher than $1400\text{ }^\circ\text{C}$ for densification. HA-Ti composites exhibited high expansion values which consequently resulted in low mechanical properties.

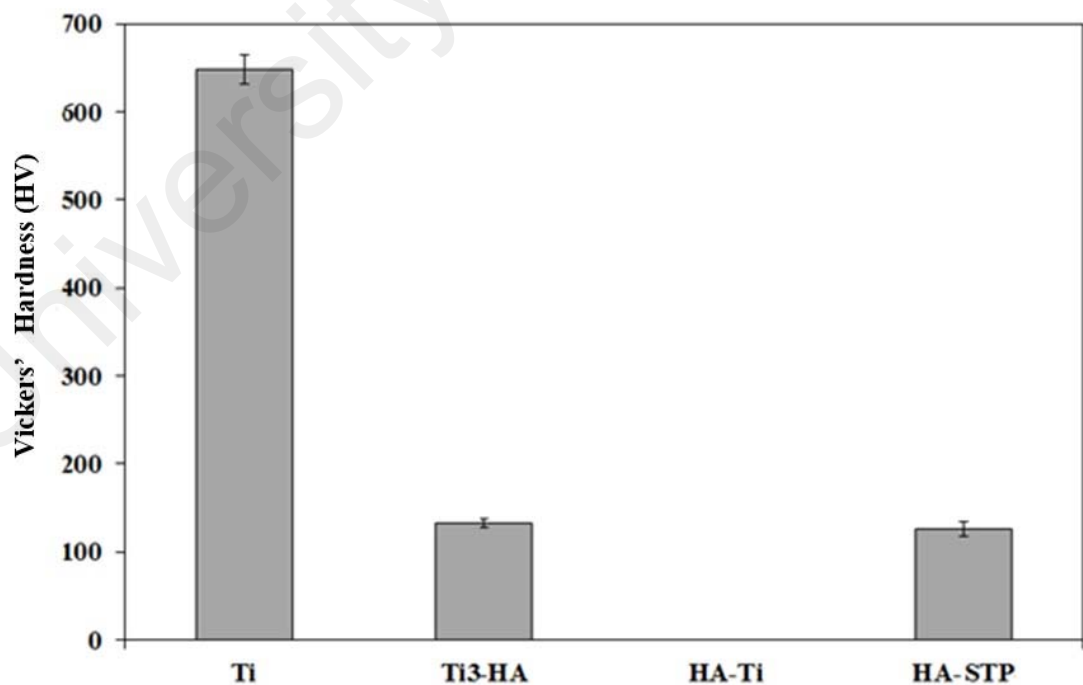


Figure 4.5. Comparison between the Vickers' hardness values of the sintered pure titanium, Ti3-HA, HA-Ti, and HA-STP composite.

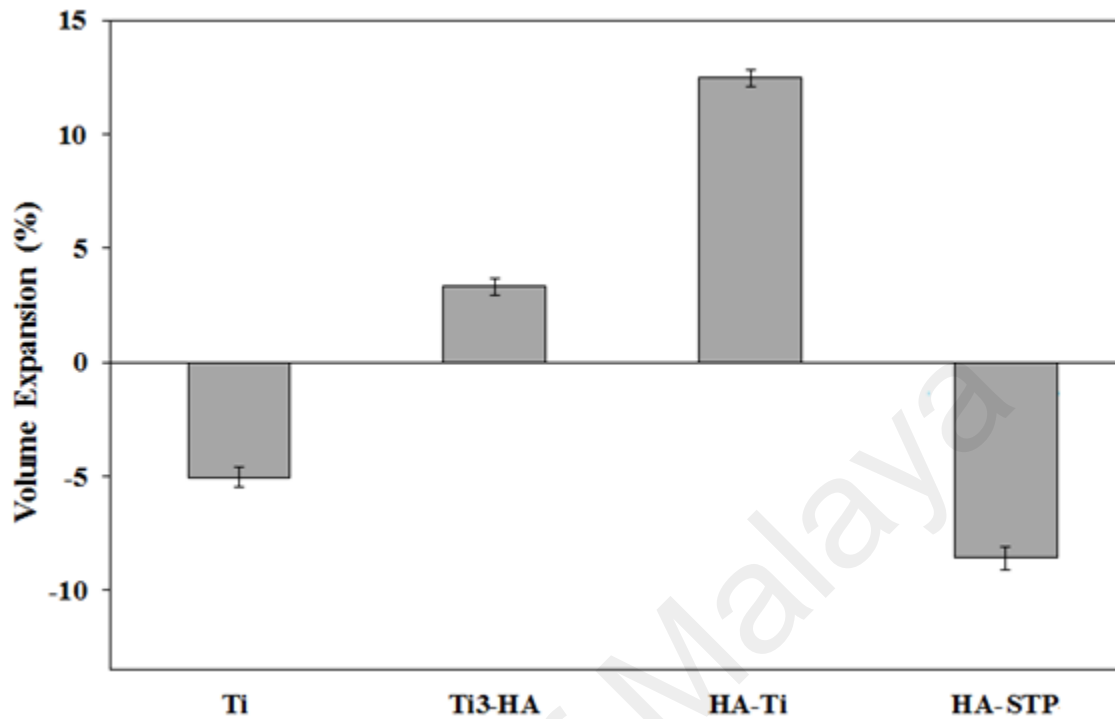


Figure 4.6. Comparison between the expansion ratios of sintered pure titanium, Ti₃-HA, HA-Ti, and HA-STP composite.

4.1.4 Volumetric Expansion of the Sintered HA-STP Single Layer

The volumetric expansion of the HA-STP composite is compared with those of pure Ti, Ti₃-HA, and HA-STP in Figure 4.6. The expansion is probably due to the significant mismatch between the crystal lattice parameters of the initial and resulting phases, which produces a large quantities of defects such as vacancies, dislocations and stacking faults at particles interfaces, thereby resulting in unpacked and fragile matrix (Brown and Epstein, 1965). Instead, the HA-STP composites exhibited a relatively high hardness value which was comparable to that of Ti₃-HA. The limited inter-phase interactions in HA-STP composites could result in more stability of the crystal lattice parameters at the interfaces. Moreover, the lattice parameters of the decomposition phases are almost

similar to that of the initial phases, producing minimum physical stresses in the HA-STP composites (Brown and Epstein, 1965).



Figure 4.7. The sintered FGM structures using (a) pure Ti, and (b) STP.

4.2 FGM Structure

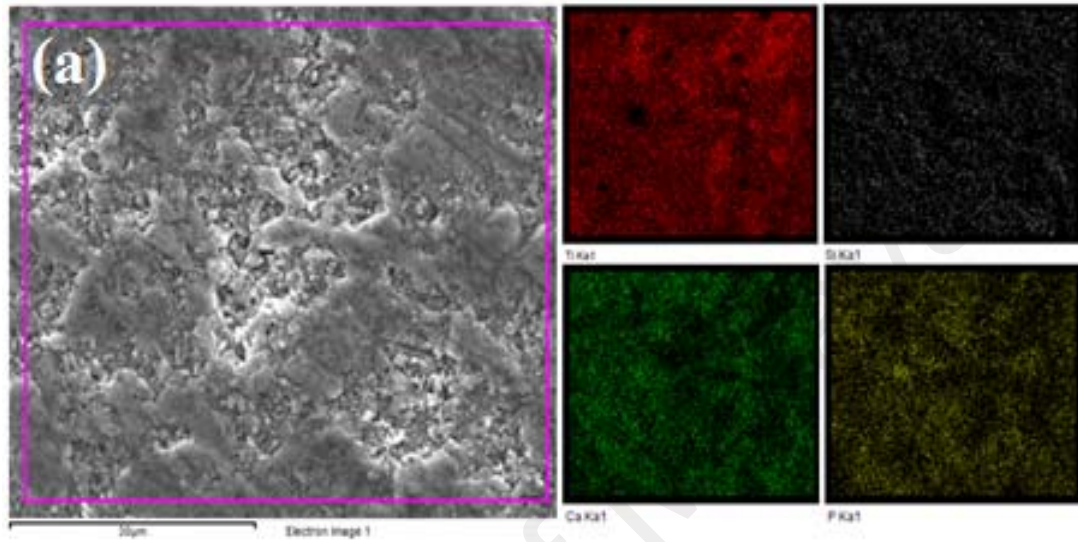
4.2.1 FGM Morphology

Figure 4.7 shows the morphology of the sintered FGM structures fabricated by pure Ti or STP. It is obvious that the FGM structure fabricated pure titanium contains many micro- and macro-cracks on its surface because of the unjustified distribution of the residual thermal stress during the fabrication process, volumetric expansion of the FGM layers, and formation of brittle phases which can deteriorate the properties of FGM (Chu *et al.*, 2001). Specifically, each composite layer had a distinct appearance depending on the volume fractions of each constituent material, possibly resulting in crack formation along interfaces due to the large differences in fracture strengths of different FGM layers. In contrast, the modified HA-STP FGM structure showed better performance with volumetric shrinkage during sintering and thus, reduced crack formation and propagation within the material. Therefore, optimization of the FGM composition by incorporation of STP powder rather than pure titanium could potentially result in less residual thermal macroscopic stress during the fabrication process, leading to better mechanical performance of the sintered graded structure when applied for fabrication of dental posts.

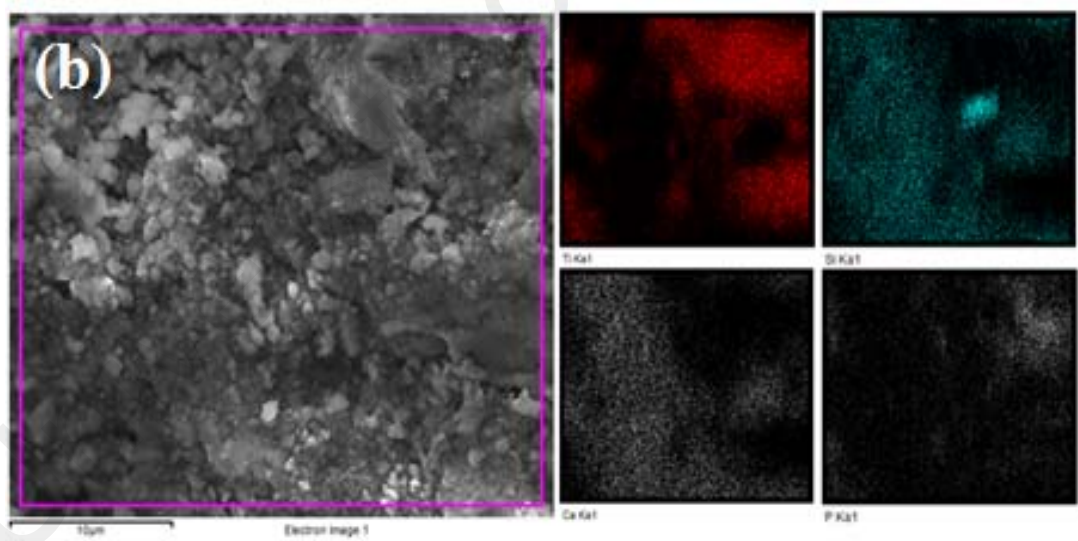
The SEM images of different FGM layers with their corresponding elemental map analyses are illustrated in Figure 4.8. The SEM images of different layers shows no evidence of cracks and silica could uniformly cover the Ti particles. This suggested that the sintering process was performed satisfactorily. The elemental maps also showed the presence of Ti, Ca, Si, and P atoms in all the FGM layers, indicating the existence of silica-coated titanium particles.

Figure 4.9 also shows the peak intensities of titanium, silicon, calcium, and phosphorus in different FGM layers. As shown in these figures, the peak intensity of Ti and Ca are

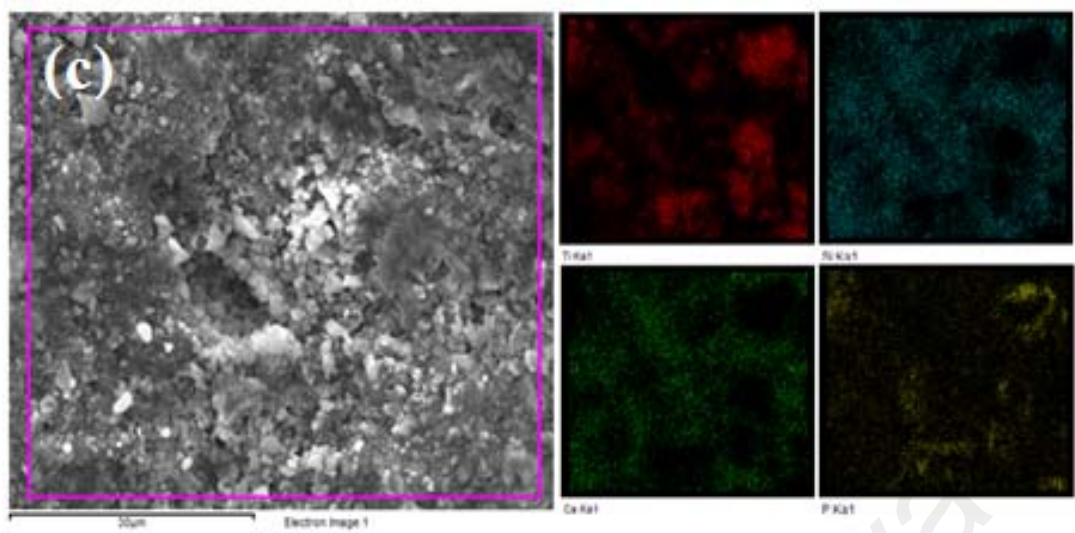
gradually changed in opposite directions within the FGM layers, which confirm the gradient alteration of the composition of these composite layers.



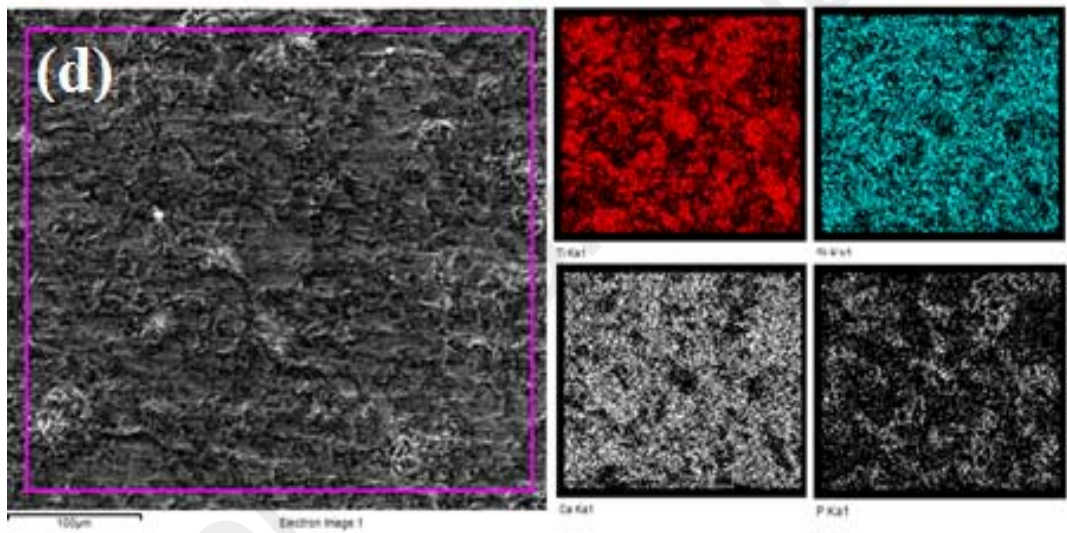
Magnification: 50μm



Magnification: 10μm



Magnification: 50µm



Magnification: 100µm

Figure 4.8. SEM Micrographs and elemental analyses of (a) 9STP-1HA, (b) 8STP-2HA, (c) 7STP-3HA, and (d) 6STP-4HA layers.

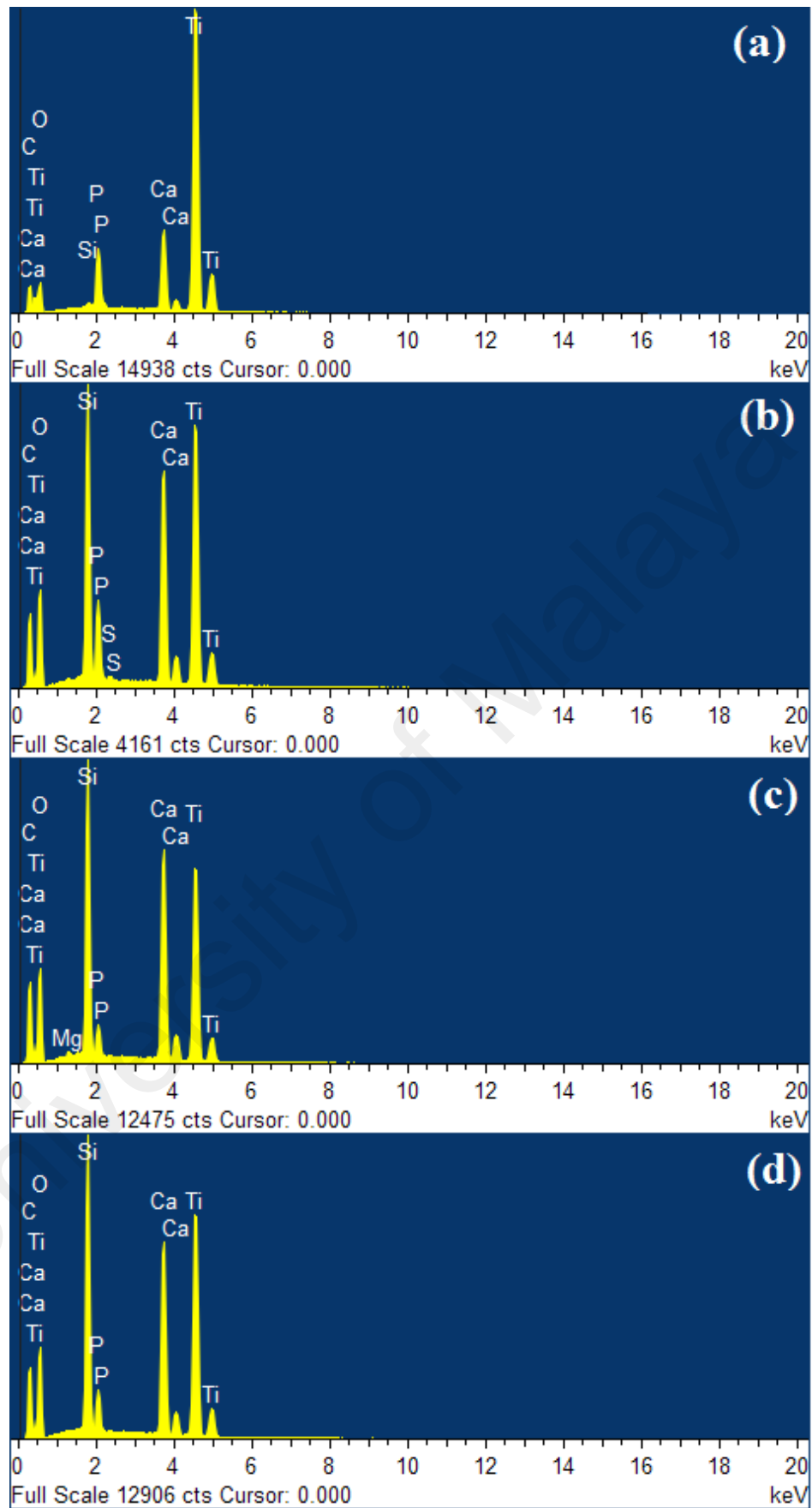


Figure 4.9. The peak intensities of Ti, Si, Ca, and P elements in (a) 9STP-1HA, (b) 8STP-2HA, (c) 7STP-3HA, and (d) 6STP-4HA layers of the FGM structure.

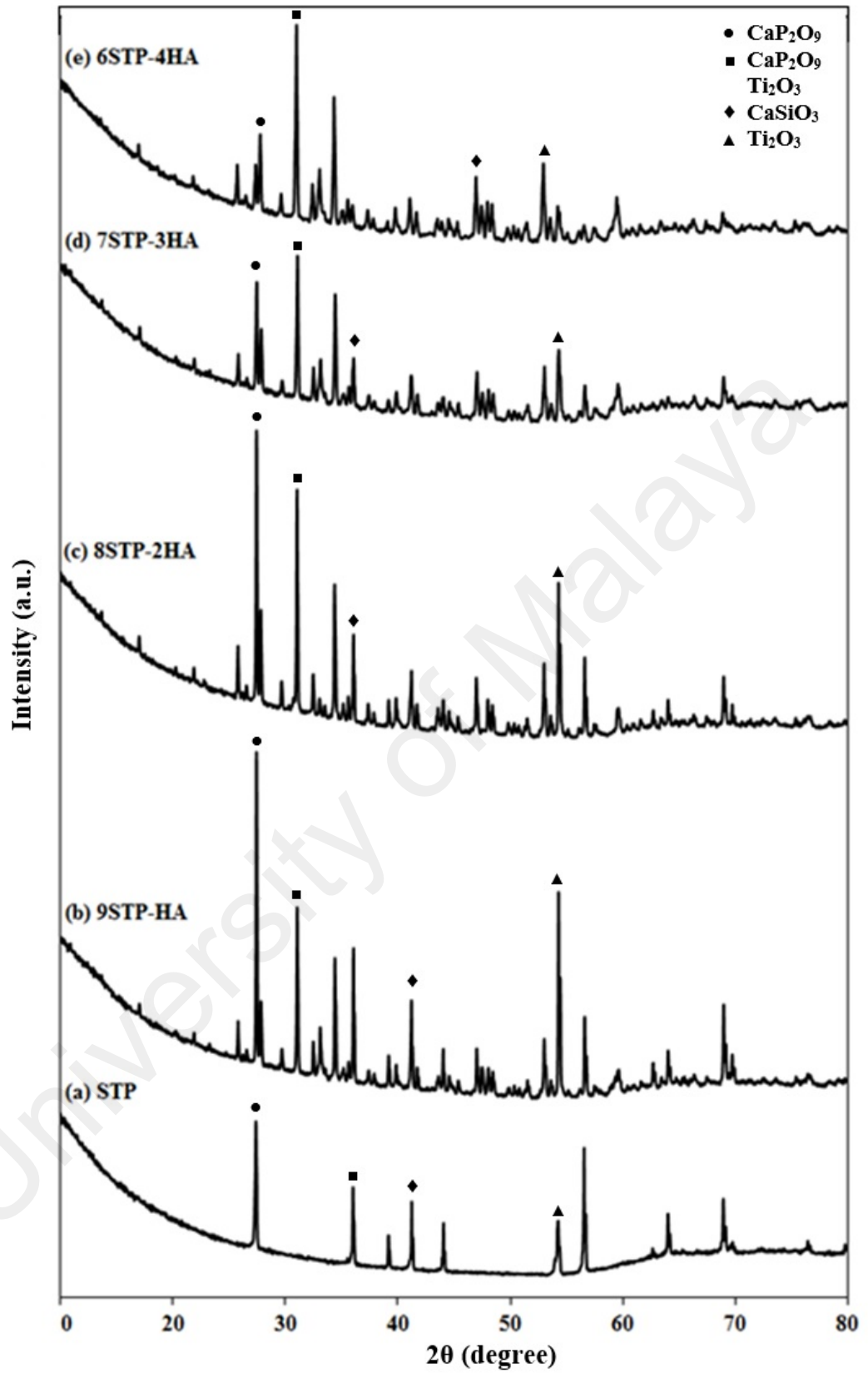


Figure 4.10. The XRD spectra of different FGM layers; (a) STP, (b) 9STP-1HA, (c) 8STP- 2HA, (d) 7STP- 3HA, and (e) 6STP-4HA.

4.2.2 Chemical Interaction of HA and STP in the FGM Layers

The phase stability and probable chemical interaction between STP and HA constituents with different weight ratios were also studied accordingly by XRD analysis. The XRD pattern of different FGM layer at angle range of 20-70 are shown in Figure 4.10. As confirmed previously, the XRD pattern of STP showed the intense peaks of Ti, indicating its stability in the basic environment prepared for the synthesis of amorphous SiO₂ coating, which is observed in the XRD peaks as a hill at low angles. The XRD spectra of different layers confirmed the gradual change of STP-HA composition from the starting layer of STP to the last layer of 6STP-4HA, with almost similar decomposition compounds in the multilayered FGM composite. The gradual change in compositions and microstructure of STP-HA is likely to lead to a gradual change in material properties.

It was reported that a presence of Ti and/or its oxides could contribute to the decomposition of HA (Weng *et al.*, 1994). HA usually decomposed to CaSiO₃, Ca₃(PO₄)₂ and H₂O. The addition of the Si to the Ti/HA composites could affect the final phases of the composite. As a result of incorporating STP instead of pure Ti, formation of undesired brittle compounds such as CaTiO₃ and Ti_xP_y. Calcium oxide phosphate (CaO) were minimized in all the FGM layers. The decomposition phases present in the FGM layers are almost identical to that of STP-HA explained previously, including titanium oxides (e.g. Ti₂O₃), calcium phosphates, CaPs (mostly CaP₂O₆) and calcium silicate (mostly CaSiO₃). The main crystalline phase of Ti which was nearly to α -Ti phase completely disappeared while dominant phases as mentioned was appeared.

The presence of SiO₂ could not fully protect against oxidation and decomposition of CaP. However, the most observed compound obtained was the formation of CaSiO₃ that could exhibit a surface chemistry that enable to extracellular matrix proteins

(Kaewsichan *et al.*, 2011). Silica acted as a nucleating apatite, in conjunction with strong protein films on the material that facilitated cell adhesion and other cellular activities to the bone/tooth bonding in vivo. The complete disappearance of HA suggested that the existence of titanium reduced the decomposition temperature of hydroxyapatite to temperatures lower than 1000 °C (CQ Ning and Zhou, 2004). Ti atoms were tend to oxidize mostly on top of Ti surface. The oxidation kinetics of titanium were determined by adsorption rate of oxygen, oxygen as an interstitial atom diffuses to the Ti lattice until reaching a saturation level, followed by oxidation of titanium (Arifin *et al.*, 2014).

4.2.3 Vickers' Microhardness of the FGM Layers

According to the rule of mixture, the Vickers' hardness value must increase when the Ti weight percentage is increased in the Ti/HA composites. However, high Ti percentages in contact with HA could drastically reduce the hardness due to formation of secondary phases during sintering. The Vickers' hardnesses of different FGM layers are compared in Figure 4.11. Although the differences of the Vickers's hardness values of adjacent layers in general were not statistically significant, the gradual raising of the STP content in the FGM layers could result in a gradient increase of their Vickers' hardness where the STP layer is significantly harder than the 6STP-4HA, 7STP-3HA, and 9STP-1HA.

The high hardness of different FGM layer containing STP instead of pure titanium is probably attributed to the minimization of the formation of some brittle phases such as calcium titanate (CaTiO_3) and Titanium phosphides (Ti_xP_y) which are generally produced when HA is in contact with pure Ti at elevated temperatures. Moreover, the desirable range of Vickers' hardness values obtained in different FGM layer indicate that the experimental temperature of 1100 °C used in this study is appropriate and reliable for densification and simultaneously retain the desirable calcium phosphate phases.

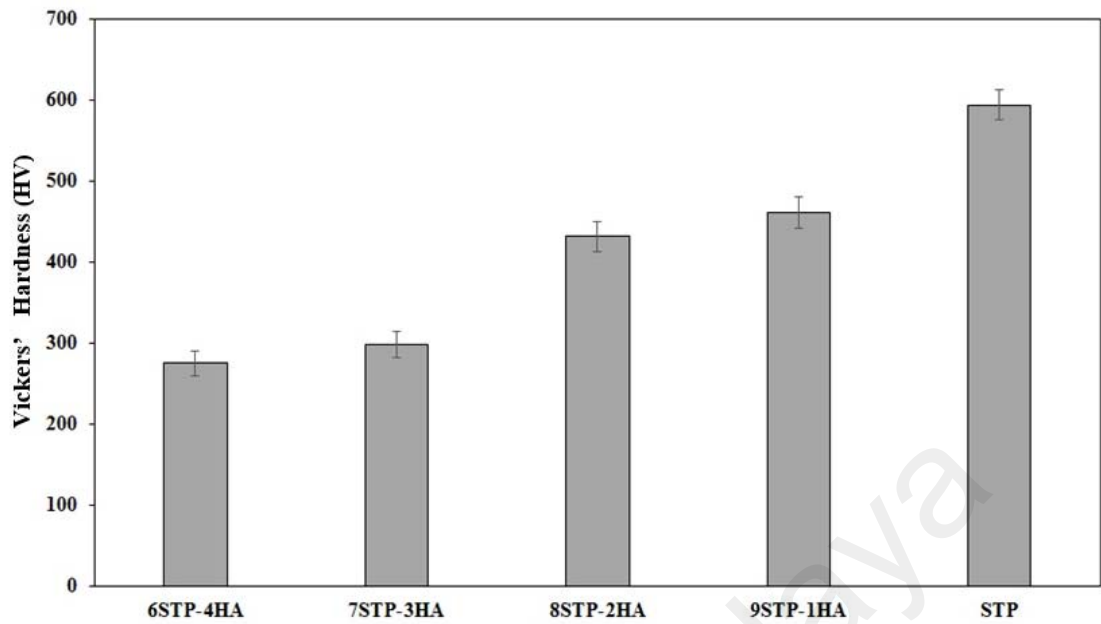


Figure 4.11. Comparison between the Vickers' hardnesses of different FGM layers.

4.2.4 Volumetric Expansion of the FGM Layers

In a similar manner to the Vickers hardness results, a gradual behavior is also observed in the volumetric shrinkage ratios of different FGM composite layers. As shown in Figure 4.12, all the FGM layers undergo volumetric shrinkage at elevated temperature, which indicate their successful sintering at the selected temperature (1100 °C). The volumetric shrinkage could probably result in reduced amounts of micro- and macro-cracks in the FGM structure when cooled to the room temperature and thus, their improved mechanical properties compared to the Ti-HA composites which drastically expand during cooling process. The volumetric shrinkage of adjacent FGM layers were not statistically different. However, from the first FGM layer to the last one, a statistically significant increase in the volumetric shrinkage is observed. It seems that increase of the STP content resulted in gradual decline of the volumetric shrinkages in the FGM layers, indicating higher tendency of HA content to sintering compared to STP at the selected sintering temperature.

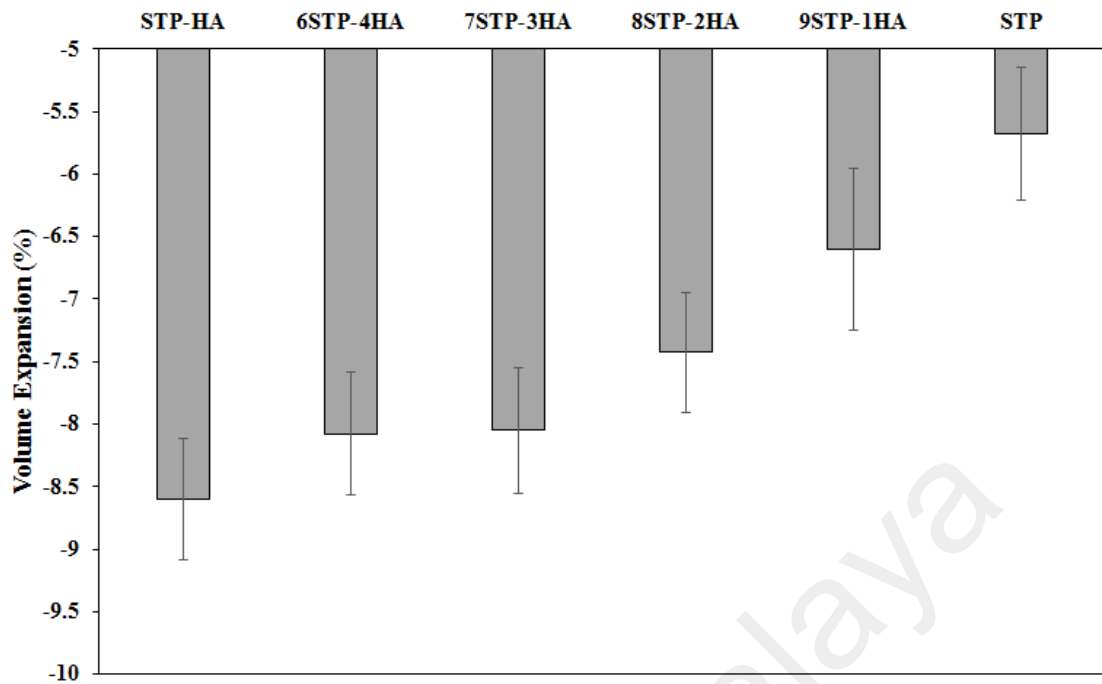


Figure 4.12. Comparison between the volumetric expansion of different FGM layers.

4.2.5 Experimental Density of the FGM Layers

The measured experimental densities for all the FGM layers as well as the STP-HA composite are plotted in Figure 4.13. For all the FGM layers, the experimental densities were significantly lower than those obtained by rule of mixture. This probably show the insufficient pressure applied in the CIP process to densify the composite layers, which resulted in high porosity in the composites microstructure. The presence of porosity could in turn drastically reduce the mechanical performance of the fabricated FGM composite. However, a gradual behaviour in the density values of different FGM layers is again observed, despite the density changes in the adjacent layers were not statistically significant. In general, increase of the HA content resulted in decline of the layer density due to its lower theoretical density compared to titanium.

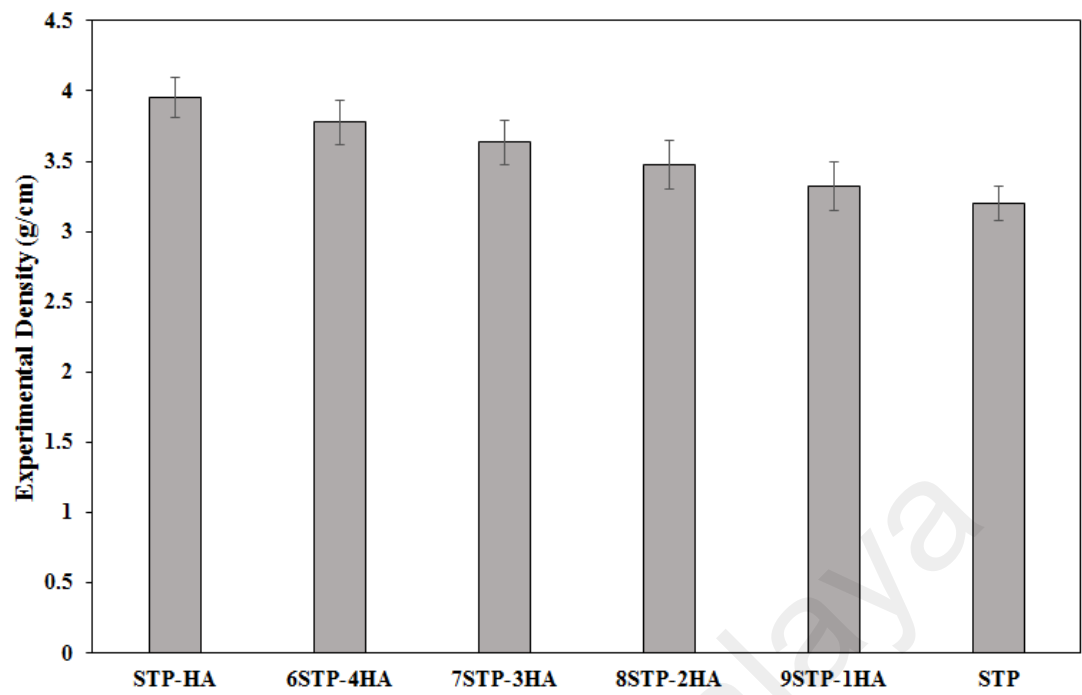


Figure 4.13. The experimental densities of different FGM layers and STP-HA composite.

Chapter 5

Discussion

Development of biomaterials with desirable mechanical properties for load-bearing application is one of the challenging tasks for materials science today. When we consider the tooth/bone implants, it is important to have variations of the material properties with location, in order to simulate the natural structure and thus, optimize the overall function of the implant. However, due to the thermal and mechanical instability of functionally graded materials, these heterogeneous composites have not been successfully used for fabrication of load-bearing implants. It is assumed that the surface modification of metallic particles used in FGM mixtures, could minimize the unfavourable metallic-ceramic interactions and result in less decomposition during sintering and better mechanical properties. The application of this technology could improve the mechanical behaviour of implants decrease the fracture risk during load application. This study was firstly focused on the surface modification of the titanium particles by a thin silica layer. These silica-coated titanium (STP) powders were assumed to have less chemical interaction with hydroxyapatite due to the high chemical stability of silica. These particles were then incorporated in the FGM composite layers and various physical, chemical, and mechanical properties of the produced FGM multilayer were characterized.

5.1 STP Synthesis

Microstructural characterization is an important feature in view of the particle size and morphology of titanium after formation of the protective silica layer. These characterizations are also important to determine the possible aggregation between the titanium particles as a result of silica formation as well as to ensure uniform coverage of the particle surfaces by this ceramic protective layer.

Comparison of the microscopic images of the Ti powder indicated a uniformity in particle size of the black-coloured Ti powder. When these particles were immersed in the strongly basic solution containing ethanol and tetraethyl orthosilicate (TEOS) is added, the powder colour was transformed from black to grey, while the solution turned to white which indicated formation of silica. The microscopic images of these particles confirmed coating of the titanium particles with an almost thin layer of silica (compared to the coarse particle size of titanium). In fact due to the large particle size of titanium, the silica coating is formed from an aggregation of numerous silica nanoparticles in the particle size of approximately 100-200 nm on the titanium surfaces. However, probably due to the irregular geometry of the Ti particles, the silica layer in some regions, particularly on the sharp edges, which probably result in increased contact between titanium and HA and further decomposition in the sintering process. Therefore, it seems that producing titanium particles with more uniform and smaller sizes could potentially result in a more even formation of the silica layer and thus, higher protection against undesirable reactions with the HA phase at sintering temperatures.

5.2 Fabrication of the Single-layer Composite

5.2.1 Ti/HA/Si Interactions

The interaction of composite ingredients can be evaluated by a number of analytical techniques such as X-ray diffraction, energy dispersive spectroscopy (EDX), Fourier transform infrared (FT-IR), Raman spectroscopy, and X-ray photoelectron spectroscopy (XPS).

The XRD pattern of the sintered HA-Ti composite (control specimen) indicated the complete removal of the initial components (HA and Ti) peaks and dominance of the

Ti_xP_y (mostly Ti₅P₃) and TiCaO₃ phases in the composite structure. This clearly showed the occurrence of undesired reaction between Ti and HA powders and formation of brittle compounds, significant increase of the volumetric expansion, and high water absorption after cooling down to the room temperature, which all drastically reduce the mechanical stability. Therefore, the resulting composite fragile, which made them inappropriate for fabrication of dental posts and other load-bearing implants. In contrast, the XRD analysis of the sintered HA-STP composite showed a more controlled chemical behaviour, causing complete removal of CaTiO₃ and Ti_xP_y. However, the presence of SiO₂ could not fully protect Ti and HA against oxidation and decomposition to Ca_xP_y phases, respectively. Due to the similarity of the diffraction peaks of different Ca_xP_y formulations (e.g. HA, oxyapatites, tetracalcium phosphate (TTCP), tricalcium phosphates (α- and β-TCP)) and overshadowing their peaks by strong peaks of Ti₂O₃, it was difficult to accurately determine the Ca_xP_y types produced in the composite. In the addition of SiO₂, calcium silicate (mostly CaSiO₃) was among the most observed compounds in the FGM layers. However, this compound may exhibit less negative impact on the mechanical properties compared to calcium titanate and titanium phosphides. According to the previous studies, calcium silicate may even show reinforcing influence on the HA matrix (Kaewsichan *et al.*, 2011).

Although X-ray diffraction is known as a versatile, non-destructive analytical technique for identification and quantitative determination of the various crystalline forms and components phases present in powdered and solid samples, this approach may not provide sufficient accuracy when concentration of a component is low. Moreover, similarity of the calcium phosphate peaks as well as their overlapping by the strong metallic peaks result in difficulties in precise determination of the phases formed during the sintering process. Therefore, utilization of FT-IR technique as a complimentary approach could help in better characterization of the composite layers and differentiation

of the calcium phosphate phases. Therefore in this study, FT-IR analysis was also employed to determine the possible phase changes and the chemical interaction between Ti and HA in the TI-HA composites (used as control specimens) as well as STP and HA in the modified composite structure.

Based on the first objective, strong peaks observed in pure HA at 963 cm^{-1} , 1021 cm^{-1} and 1087 cm^{-1} represented the phosphate (PO_4^{3-}) band, while the weak peak at 3571 cm^{-1} showed the hydroxyl (OH^-) group which is characteristic band of the HA structure. In the FT-IR spectrum of the STPs, all the absorption peaks represented the Si-O band. For the calcinated HA-STP, the silane and phosphate peaks were clearly observed. However, due to a low SiO_2/HA ratio, the silane vibration at 1058 cm^{-1} was overlapped by the phosphate principal peaks.

For sintered HA-Ti, the FT-IR spectrum indicated the elimination of phosphate peaks due to the complete removal of HA during the sintering process. This spectrum was actually similar to that of pure CaO mentioned in the previous studies (Ye *et al.*, 2009). It shown that peaks at 873 cm^{-1} and $1400\text{-}1600\text{ cm}^{-1}$ corresponded to the C-O band, while the short peak at 3634 cm^{-1} represented the Ca-O-H vibration. The carbonate band showed the formation of CaCO_3 to the integration of CaO with CO_2 absorbed during handling and sample preparation (Ye *et al.*, 2009). The elimination of PO_4^{3-} bands demonstrated the complete decomposition of Ca_xP_y phases to an amorphous phase and CaO which further resulted in formation of CaTiO_3 and CaCO_3 .

In the HA-STP composite, the phosphate peaks at 940 cm^{-1} and 970 cm^{-1} were clearly observed, demonstrating the presence of Ca_xP_y phases. However, the phosphate peaks were different from those of pure HA or oxyapatite (dehydroxylated HA) and fitted with those of β -TCP (Meejoo *et al.*, 2006). The sharp peak at 710 cm^{-1} also represented the Ti-O band, while the broad peaks at 820 cm^{-1} and 1600 cm^{-1} were respectively, attributed to

the Si-O band of amorphous silica and Si-O-Ca vibration, indicating the formation of calcium silicate. Although the results showed the existence of decomposition of HA and oxidation of Ti during the sintering process at 1100°C, however, the undesired interactions between HA and Ti components were minimized, causing complete removal of calcium titanate and titanium phosphides as well as formation of stable calcium phosphates in the sintered composite.

5.2.2 Mechanical Performance

The mechanical behavior of the composite was evaluated by Vickers' microhardness test. Moreover, the volumetric expansion (or shrinkage) of the composites were also quantified as a significant indicator of the mechanical stability after completion of the sintering process. Maximum sintering temperature, sintering time at maximum temperature, and heating/cooling rates are among the most crucial parameter during sintering of the compositions prepared by powder metallurgy. In general, low sintering temperatures and insufficient sintering times could result in inefficient fusion of the particles and low densification of the composite, which further result in low mechanical strength. Moreover, improper cooling rates may also lead to rapid expansion of the composite ingredients. Consequently, due to the different expansion ratios of the constituents, several micro- and macro-cracks may be generated within the composite structure, which drastically decrease the mechanical performance. Therefore, a desirable sintering protocol must result in high densification (high volumetric shrinkage), reduced interparticle porosities, and minimization of the crack formation in the microstructure.

Formation of brittle phases in the Ti-HA composites was such considerable that the specimens could not even tolerate the gentle forces applied during the microhardness

tests. Numerous cracks were apparent on the composite surfaces, which could be seen without using any imaging instrument. As mentioned previously, the low hardness of HA-Ti samples was probably attributed to the presence of brittle phases (TiCaO_3 and Ti_xP_y) which require temperatures higher than 1400 °C for densification. HA-Ti composites exhibited high expansion values which consequently resulted in low mechanical properties. This expansion is probably due to the significant mismatch between the crystal lattice parameters of the initial and resulting phases, which produces a large quantities of defects such as vacancies, dislocations and stacking faults at particles, thereby resulting in unpacked and fragile matrix (Brown and Epstein, 1965). Instead, the HA-STP composites exhibited a relatively high hardness value which was comparable to that of composites containing 75 wt.% Ti and 25 wt.% HA. The limited inter-phase interactions in HA-STP composites could result in more stability of the crystal lattice parameters at the interfaces. Moreover, the lattice parameters of the decomposition phases are almost similar to that of the initial phases, producing minimum physical stresses in the HA-STP composites (Brown and Epstein, 1965).

5.3 FGM Design

5.3.1 Fabrication Protocol

In addition to incorporation of STP powder as an alternative to pure Ti to the composites mixture, a number of other modifications were also carried out in the fabrication process. As the first modification, the interfaces between various FGM layers were removed to minimize the negative effects resulted from the contact of layers with differed physical properties. For this aim, rather than gentle compressing of each layer after pouring its powder into the mold, all the layers were pressed in a single step after all

the layers' powders were poured into the mold. This allowed in partial interpenetration of the FGM layers and removal of the observable borders between them.

The second modification was performed by insertion of the layers' ingredients into a flexible plastic tube rather than directly pouring into the stainless steel mold. This approach resulted in reduced contamination of the FGM powder by the lubricating materials, insertion of all the layers' powders and compressing them simultaneously and gentle pressing of the powder until reaching a powder height approximately to the height of stainless steel mold and ready for the hydraulic press, as well as facile removal of the tube from the mold after hydraulic pressing.

The third modification was using conventional furnaces with normal atmosphere instead of tube furnaces with argon/nitrogen or vacuum environments. In addition to a significant reduction of the sintering cost, utilization of the normal atmosphere led to reduced tendency of hydroxyapatite due to the presence of water in the environment. Moreover, by using the air atmosphere, the change in the composite color was avoided, which possibly improve the esthetic characteristics of the fabricated dental posts. As shown previously, the produced FGM layers retained their original colors after the sintering process.

5.3.2 Chemical analysis

The chemical structure of various FGM layers was also investigated via XRD analysis to determine if the changes in the weight ratios could affect the intensity and nature of the chemical reactions between the composite constituents. The obtained results indicated that the decomposition phases observed in the XRD pattern of STP-HA single-layer such as calcium phosphates, calcium silicate, and metallic oxides, were present in the

composition of different FGM layers but with different quantities. The Ti phase could retain its stability on the strong basic condition. However, this metallic phase underwent oxidation during the sintering process and transformed to Ti_2O_3 . The intensity of titanium oxide peaks was gradually decreased by reducing the STP content while the Ca_xP_y phases become more dominant, indicating the gradient structure of the FGM multilayered composite. The presence of a compositional gradient was further confirmed by EDX analysis.

5.3.3 Mechanical Performance

As a result of compositional gradient in the FGM structure, a gradual increase of the Vickers' microhardness was observed from the 6STP-4HA to the STP layer. Although the differences of the Vickers' microhardness values between the adjacent layers were not mostly significant, the obtained results showed an approximately 115% increase in the mean Vickers' hardness of the multilayered composite when the STP concentration was increased from 60 wt.% to 100 wt.%. This indicated a successful development of gradient mechanical properties in the multilayered composite structure.

Measurement of the volumetric expansion/shrinkage of various FGM layers showed that all these composites undergo shrinkage during the sintering and cooling processes. This in turn confirms successful densification of the FGM layers via the sintering technique. Moreover, densification of the FGM layers confirmed the reduced formation of brittle compounds which generally lead to composite expansion and generation of micro- and macro-cracks in the multilayered composite. The volumetric shrinkage was gradually increased by reducing the STP content, probably due to the relatively higher temperatures required for sintering of Ti in contrast to the HA phase.

A similar gradual behavior was also observed in the experimental density of the FGM layers with increasing trend from the layers with low to high STP content. This is due to the significantly higher density of pure titanium compared to hydroxyapatite. However, by comparison of the obtained experimental densities of various composite layers with their theoretical densities measured by the rule of mixture, it was found that the experimental densities of all the composite layers were significantly less than their theoretical values. This may be due to insufficient compressing of the green powder during the hydraulic and cold isostatic presses, which leave a high interparticle porosity in the composite layers. Therefore, it is assumed that by using the CIP machines which allow reaching higher pressure values, lower porosities and higher densifications could be achieved in the FGM structure.

Chapter 6

Conclusion

The present study was categorized into two objectives including synthesis of silica-coated titanium particles (STP), and fabrication of FGM structures using hydroxyapatite (HA) and the as-synthesized STP.

6.1 STP Synthesis

1. The microscopic images of the synthesized STP confirmed coating of the Ti particles with a thin silica layer. The silica layer consisted of large aggregations of the silica nanoparticles with particle size range from 100 nm to 200 nm on surfaces of the coarse titanium microparticles.
2. However, formation of the silica layer was less uniform on the sharp edges of the titanium particles. The chemical behaviour of the HA-STP composite was relatively more controllable in contrast to the HA-Ti composites, resulting in complete elimination brittle compounds such as CaTiO_3 and Ti_xP_y .
3. The Ti oxidation and HA decomposition by incorporation of the STP powder were not fully avoided. However, the decomposition products in the STP-HA composites such as titanium oxide (i.e. Ti_2O_3), calcium silicate (CaSiO_3), and tricalcium phosphates (TCP) phases generally led to reduced negative effect on the mechanical stability of the composite.

4. Incorporation of STP instead of Ti in the composite could result in significant improvement of the Vickers' microhardness. The obtained microhardness value of the STP-HA composite was approximately identical to that of composites containing 75 wt.% titanium and 25 wt.% hydroxyapatite. In contrast, the composites produced with pure titanium could not even tolerate the gentle pressures required for performing the Vickers' microhardness experiments.
5. Measurement of the volumetric changes of the STP-HA indicated their considerable shrinkage, which confirmed their densification by the applied sintering process. This in turn could reduce formation of the micro- and macro-cracks within the composite microstructure, leading to improved mechanical characteristics and decreased fracture risk during load application.

6.2 Fabrication of the FGM Structure

1. The optimized technique employed for fabrication of the FGM structure led to elimination of the interlayer borders and thus, reduce the fracture susceptibility at these regions due to the differed physical and mechanical properties of these composite layers. Morphological investigations indicated reduced formation of the macro- and micro-cracks within the FGM structure in contrast to those fabricated using pure titanium powder.
2. The sintering protocol used in this study also retained the original appearance of the composite ingredients which is important from the esthetics point-of-view.

3. The decomposition phases such as titanium oxide, tricalcium phosphate, and calcium silicate, which were present in the STP-HA single-layer composite, were also detected in all the FGM layers but with different quantities, confirming the gradient chemical composition of the fabricated FGM structure.
4. The compositional gradient of the FGM multilayered structure also led to a gradient in the mechanical properties (i.e. Vickers' microhardness). An approximately 120% increase in the microhardness value was observed by increase of the STP concentration from 60 wt.% to 100 wt.% in the composite, indicating a successful formation of the gradient mechanical characteristics in the FGM structure.
5. The sintering process could result in volumetric shrinkage of all the FGM layers while the shrinkage was proportional to the hydroxyapatite content, probably due to its lower sintering temperature compared to metallic titanium. As mentioned, this shrinkage could result in minimization of the crack formation within the multilayered composite structure.
6. A gradient behavior was also observed in the experimental densities of various FGM layers with, where higher titanium contents result in increased experimental densities. However, the experimental values of all the FGM layers were significantly lower than their theoretical values, which indicate the insufficiency of the forces applied during the hydraulic and especially cold isostatic presses.

7. Due to their desirable mechanical properties, the developed FGM composites show potential in fabrication of load-bearing heterogeneous implants such as dental posts.

University of Malaya

Chapter 7

Recommendation for further studies

7.1 Further Studies

1. The fabrication processes of the developed FGM structure must further be optimized to achieve the mass production capability of dental posts in sophisticated geometries, which are clinically applicable in restorative dentistry.
2. Utilization of the finite element analysis (FEA) may allow in precise prediction of the performance of fabricated dental posts within the endodontically-treated teeth. The obtained results could then be employed in optimization of the post geometry and structure.
3. Further in-vitro investigations on the developed dental posts are then needed for evaluation of their biocompatibility and bioactivity. They must also further undergo in-vivo investigations for more realistic evaluation of their mechanical performance.
4. Incorporation of low-melting-point biocompatible additives as binders to the composite mixture could further result in decreased sintering temperature and higher stability of the hydroxyapatite content. This approach could also greatly reduce the fabrication cost by lowering the sintering temperature which provides sufficient composite densification.
5. The FGM structures could also be fabricated with flowable composite resins and different metallic compounds such as titanium and iron oxide particles. This approach could completely eliminate the necessity of performing costly and time-consuming sintering process.

References

- Abdulmunem, M., Dabbagh, A., Abdullah, H., & Kasim, N. H. A. (2015). The combined effect of dental post and cement materials on fracture resistance and fracture mode of endodontically-treated teeth. *Sains Malaysiana*, 44(4), 1189-1194.
- Abu Kasim, N. H., Madfa, A. A., Hamdi, M., & Rahbari, G. R. (2011). 3D-FE analysis of functionally graded structured dental posts. *Dental Materials Journal*, 30(6), 869-880.
- Al-Sanabani, J. S., Madfa, A. A., & Al-Sanabani, F. A. (2013). Application of calcium phosphate materials in dentistry. *International Journal of Biomaterials*.
- Al-Sarraf, M., Martz, K., Herskovic, A., Leichman, L., Brindle, J., Vaitkevicius, V., Emami, B. (1997). Progress report of combined chemoradiotherapy versus radiotherapy alone in patients with esophageal cancer: an intergroup study. *Journal of Clinical Oncology*, 15(1), 277-284.
- Al-Wahadni, A. M., Hamdan, S., Al-Omiri, M., Hammad, M. M., & Hatamleh, M. M. (2008). Fracture resistance of teeth restored with different post systems: in vitro study. *Oral Surgery, Oral Medicine, Oral Pathology, Oral Radiology, and Endodontology*, 106(2), e77-e83.
- Arifin, A., Sulong, A. B., Muhamad, N., Syarif, J., & Ramli, M. I. (2014). Material processing of hydroxyapatite and titanium alloy (HA/Ti) composite as implant materials using powder metallurgy: A review. *Materials & Design*, 55, 165-175.
- Assif, D., Bitenski, A., Pilo, R., & Oren, E. (1993). Effect of post design on resistance to fracture of endodontically treated teeth with complete crowns. *The Journal of Prosthetic Dentistry*, 69(1), 36-40.
- Balbinotti, P., Gemelli, E., Buerger, G., Lima, S. A. d., Jesus, J. d., Camargo, N. H. A., Soares, G. D. d. A. (2011). Microstructure development on sintered Ti/HA biocomposites produced by powder metallurgy. *Materials Research*, 14(3), 384-393.
- Besinis, A., De Peralta, T., & Handy, R. D. (2014). The antibacterial effects of silver, titanium dioxide and silica dioxide nanoparticles compared to the dental disinfectant chlorhexidine on *Streptococcus mutans* using a suite of bioassays. *Nanotoxicology*, 8(1), 1-16.
- Borum, L., & Wilson, O. (2003). Surface modification of hydroxyapatite. Part II. Silica. *Biomaterials*, 24(21), 3681-3688.
- Brown, W., & Epstein, E. F. (1965). Crystallography of tetracalcium phosphate. *Journal Res Nat Bur Stand*, 69, 547-551.
- Bruschi, M., Steinmüller-Nethl, D., Goriwoda, W., & Rasse, M. (2015). Composition and Modifications of Dental Implant Surfaces. *Journal of Oral Implants*, 2015, 14.
- Bruschi, M., Steinmüller-Nethl, D., Goriwoda, W., & Rasse, M. (2015). Composition and Modifications of Dental Implant Surfaces. *Journal of Oral Implants*, 2015.

- Cao, W., & Hench, L. L. (1996). Bioactive materials. *Ceramics International*, 22(6), 493-507.
- Chang, B.-S., Hong, K.-S., Youn, H.-J., Ryu, H.-S., Chung, S.-S., & Park, K.-W. (2000). Osteoconduction at porous hydroxyapatite with various pore configurations. *Biomaterials*, 21(12), 1291-1298.
- Chapman, B. D. (2006). *Characterization of Functionally Graded Materials*. Retrieved from (No. Afit/Gae/Eny/06-M05). Air Force Inst of Tech Wright-Patterson AFB OH Dept of Aeronautics and Astronautics.
- Chen, Y., & Fok, A. (2014). Stress distributions in human teeth modeled with a natural graded material distribution. *Dental Materials*, 30(12), e337-e348.
- Cheng, S. (2015). Research on the development and application of physical materials. Paper presented at the *First International Conference on Information Sciences, Machinery, Materials and Energy*. Atlantis Press.
- Cheng, Z., Zhang, G., Wang, Y., & Bobaru, F. (2015). A peridynamic model for dynamic fracture in functionally graded materials. *Composite Structures*, 133, 529-546.
- Chenglin, C., Jingchuan, Z., Zhongda, Y., & Shidong, W. (1999). Hydroxyapatite-Ti functionally graded biomaterial fabricated by powder metallurgy. *Materials Science and Engineering: A*, 271(1), 95-100.
- Chu, C., Xue, X., Zhu, J., & Yin, Z. (2006). Fabrication and characterization of titanium-matrix composite with 20 vol% hydroxyapatite for use as heavy load-bearing hard tissue replacement. *Journal of Materials Science: Materials in Medicine*, 17(3), 245-251.
- Chu, C., Zhu, J., Yin, Z., & Lin, P. (2001). Structure optimization and properties of hydroxyapatite-Ti symmetrical functionally graded biomaterial. *Materials Science and Engineering: A*, 316(1), 205-210.
- Dorozhkin, S. (2007). Bioceramics based on calcium orthophosphates (Review). *Glass and Ceramics*, 64(11-12), 442-447.
- Dorozhkin, S. V., & Epple, M. (2002). Biological and medical significance of calcium phosphates. *Angewandte Chemie International Edition*, 41(17), 3130-3146.
- Elias, C. N., Oshida, Y., Lima, J. H. C., & Muller, C. A. (2008). Relationship between surface properties (roughness, wettability and morphology) of titanium and dental implant removal torque. *Journal of the Mechanical Behavior of Biomedical Materials*, 1(3), 234-242.
- Erdogan, F. (1995). Fracture Mechanics of Functionally Graded Materials. *MRS Bulletin*, 20(01), 43-44.

- Fernandes, A. S., & Dessai, G. S. (2001). Factors Affecting the Fracture Resistance of Post-Core Reconstructed Teeth: A Review. *International Journal of Prosthodontics*, 14(4), 355-363.
- Fernandes, A. S., Shetty, S., & Coutinho, I. (2003). Factors determining post selection: a literature review. *The Journal of Prosthetic Dentistry*, 90(6), 556-562.
- Guo, L.-C., & Noda, N. (2007). Modeling method for a crack problem of functionally graded materials with arbitrary properties—piecewise-exponential model. *International Journal of Solids and Structures*, 44(21), 6768-6790.
- Gupta, A., & Talha, M. (2015). Recent development in modeling and analysis of functionally graded materials and structures. *Progress in Aerospace Sciences*, 79, 1-14.
- Hanprasopwattana, A., Rieker, T., Sault, A. G., & Datye, A. K. (1997). Morphology of titania coatings on silica gel. *Catalysis Letters*, 45(3-4), 165-175.
- Hedia, H., & Mahmoud, N.-A. (2004). Design optimization of functionally graded dental implant. *Bio-Medical Materials and Engineering*, 14(2), 133-143.
- Helal, W., & Shi, D. (2016). *Optimum material gradient for a Functionally Graded Endodontic Prefabricated Post: FEA*. Paper presented at the Advanced Materials, Mechanical and Structural Engineering: Proceedings of the 2nd International Conference of Advanced Materials, Mechanical and Structural Engineering (AMMSE 2015), Je-ju Island, South Korea, September 18-20, 2015.
- Heydecke, G., Butz, F., & Strub, J. R. (2001). Fracture strength and survival rate of endodontically treated maxillary incisors with approximal cavities after restoration with different post and core systems: an in-vitro study. *Journal of Dentistry*, 29(6), 427-433.
- Hing, K. A., Revell, P. A., Smith, N., & Buckland, T. (2006). Effect of silicon level on rate, quality and progression of bone healing within silicate-substituted porous hydroxyapatite scaffolds. *Biomaterials*, 27(29), 5014-5026.
- Höland, W., Rheinberger, V., Apel, E., Ritzberger, C., Rothbrust, F., Kappert, H., Nesper, R. (2009). Future perspectives of biomaterials for dental restoration. *Journal of the European Ceramic Society*, 29(7), 1291-1297.
- Howard, S., Tsui, Y., & Clyne, T. (1994). The effect of residual stresses on the debonding of coatings—I. A model for delamination at a bimaterial interface. *Acta Metallurgica et Materialia*, 42(8), 2823-2836.
- Huang, M., Rahbar, N., Wang, R., Thompson, V., Rekow, D., & Sboyejo, W. (2007). Bioinspired design of dental multilayers. *Materials Science and Engineering: A*, 464(1), 315-320.
- Hunter, A., Feiglin, B., & Williams, J. (1989). Effects of post placement on endodontically treated teeth. *The Journal of Prosthetic Dentistry*, 62(2), 166-172.

- Jean, A., Kerebel, B., Kerebel, L.-M., Legeros, R. Z., & Hamel, H. (1988). Effects of various calcium phosphate biomaterials on reparative dentin bridge formation. *Journal of Endodontics*, 14(2), 83-87.
- Kaewsichan, L., Riyapana, D., Prommajana, P., & Kaewsrichan, J. (2011). Effects of sintering temperatures on micro-morphology, mechanical properties, and bioactivity of bone scaffolds containing calcium silicate. *Science Asia*, 37, 240-246.
- Khor, K., Gu, Y., Quek, C., & Cheang, P. (2003). Plasma spraying of functionally graded hydroxyapatite/Ti-6Al-4V coatings. *Surface and Coatings Technology*, 168(2), 195-201.
- King, P., & Setchell, D. (1990). An in vitro evaluation of a prototype CFRC prefabricated post developed for the restoration of pulpless teeth. *Journal Oral Rehabilitation*, 17(6), 599-609.
- Knowles, J., Talal, S., & Santos, J. (1996). Sintering effects in a glass reinforced hydroxyapatite. *Biomaterials*, 17(14), 1437-1442.
- Kumar, R. R., & Wang, M. (2002). Functionally graded bioactive coatings of hydroxyapatite/titanium oxide composite system. *Materials Letters*, 55(3), 133-137.
- Leyens, C., & Peters, M. (2003). *Titanium and titanium alloys*: Wiley Online Library.
- Liu, X., Chu, P. K., & Ding, C. (2004). Surface modification of titanium, titanium alloys, and related materials for biomedical applications. *Materials Science and Engineering: R: Reports*, 47(3), 49-121.
- Lynn, A., & DuQuesnay, D. (2002). Hydroxyapatite-coated Ti-6Al-4V: Part 1: the effect of coating thickness on mechanical fatigue behaviour. *Biomaterials*, 23(9), 1937-1946.
- Mahamood, R. M., Akinlabi, E. T., Shukla, M., & Pityana, S. (2012). *Functionally graded material: an overview*.
- Meejoo, S., Maneeprakorn, W., & Winotai, P. (2006). Phase and thermal stability of nanocrystalline hydroxyapatite prepared via microwave heating. *Thermochimica Acta*, 447(1), 115-120.
- Miyamoto, Y., Kaysser, W., Rabin, B., Kawasaki, A., & Ford, R. G. (2013). *Functionally graded materials: design, processing and applications* (Vol. 5): Springer Science & Business Media.
- Morks, M., Fahim, N., & Kobayashi, A. (2008). Structure, mechanical performance and electrochemical characterization of plasma sprayed SiO₂/Ti-reinforced hydroxyapatite biomedical coatings. *Applied Surface Science*, 255(5), 3426-3433.

- Naderi, S., Dabbagh, A., Hassan, M. A., Razak, B. A., Abdullah, H., & Kasim, N. H. A. (2016). Modeling of porosity in hydroxyapatite for finite element simulation of nanoindentation test. *Ceramics International*, 42(6), 7543-7550.
- Niinomi, M. (1998). Mechanical properties of biomedical titanium alloys. *Materials Science and Engineering: A*, 243(1-2), 231-236.
- Ning, C., & Zhou, Y. (2004). On the microstructure of biocomposites sintered from Ti, HA and bioactive glass. *Biomaterials*, 25(17), 3379-3387.
- Ning, C., & Zhou, Y. (2008). Correlations between the in vitro and in vivo bioactivity of the Ti/HA composites fabricated by a powder metallurgy method. *Acta Biomaterialia*, 4(6), 1944-1952.
- Obbineni, M. R. (2013). *Dynamic stability analysis of a sandwich beam with functionally graded material constraining layer*. National Institute of Technology Rourkela.
- Ottl, P., Hahn, L., Lauer, H. C., & Fay, M. (2002). Fracture characteristics of carbon fibre, ceramic and non-palladium endodontic post systems at monotonously increasing loads. *Journal Oral Rehabilitation*, 29(2), 175-183.
- Peroz, I., Blankenstein, F., Lange, K.-P., & Naumann, M. (2005). Restoring endodontically treated teeth with posts and cores—a review. *Quintessence Int*, 36(9), 737-746.
- Rivera-Muñoz, E. M. (2011). *Hydroxyapatite-based materials: synthesis and characterization* (Vol. 4): INTECH Open Access Publisher.
- Ruys, A., Wei, M., Sorrell, C., Dickson, M., Brandwood, A., & Milthorpe, B. (1995). Sintering effects on the strength of hydroxyapatite. *Biomaterials*, 16(5), 409-415.
- Sadjadi, M. S., Ebrahimi, H. R., Meskinfam, M., & Zare, K. (2011). Silica enhanced formation of hydroxyapatite nanocrystals in simulated body fluid (SBF) at 37 °C. *Materials Chemistry and Physics*, 130(1-2), 67-71.
- Sadollah, A., & Bahreininejad, A. (2012). *Optimum functionally gradient materials for dental implant using simulated annealing*: INTECH Open Access Publisher.
- Sakkers, R., Dalmeyer, R., Brand, R., Rozing, P., & Van Blitterswijk, C. (1997). Assessment of bioactivity for orthopedic coatings in a gap-healing model. *Journal of Biomedical Materials Research*, 36(2), 265-273.
- Schwartz, R. S., & Robbins, J. W. (2004). Post Placement and Restoration of Endodontically Treated Teeth: A Literature Review. *Journal of Endodontics*, 30(5), 289-301.
- Shahrjerdi, A., Mustapha, F., Bayat, M., Sapuan, S., & Majid, D. (2011). Fabrication of functionally graded hydroxyapatite-titanium by applying optimal sintering procedure and powder metallurgy. *International Journal of the Physical Sciences*, 6(9), 2258-2267.

- Shaw, L. L. (1998). Thermal residual stresses in plates and coatings composed of multi-layered and functionally graded materials. *Composites Part B: Engineering*, 29(3), 199-210.
- Shirliff, V., & Hench, L. (2003). Bioactive materials for tissue engineering, regeneration and repair. *Journal of Materials Science*, 38(23), 4697-4707.
- Sidoli, G. E., King, P. A., & Setchell, D. J. (1997). An in vitro evaluation of a carbon fiber-based post and core system. *The Journal of Prosthetic Dentistry*, 78(1), 5-9.
- Silverstein, W. H. (1964). The reinforcement of weakened pulpless teeth. *The Journal of Prosthetic Dentistry*, 14(2), 372-381.
- Sola, A., Bellucci, D., Cannillo, V., & Cattini, A. (2011). Bioactive glass coatings: a review. *Surface Engineering*, 27(8), 560-572.
- Tampieri, A., Celotti, G., Sprio, S., & Mingazzini, C. (2000). Characteristics of synthetic hydroxyapatites and attempts to improve their thermal stability. *Materials Chemistry and Physics*, 64(1), 54-61.
- Tonsuaadu, K., Gross, K. A., Plūduma, L., & Veiderma, M. (2011). A review on the thermal stability of calcium apatites. *Journal of Thermal Analysis and Calorimetry*, 110(2), 647-659.
- Torbjörner, A., & Fransson, B. (2004). A literature review on the prosthetic treatment of structurally compromised teeth. *International Journal of Prosthodontics*, 17(3).
- Trabert, K., Caputo, A., & Abou-Rass, M. (1978). Tooth fracture\ 3-A comparison of endodontic and restorative treatments. *Journal of Endodontics*, 4(11), 341-345.
- Traini, T., Mangano, C., Sammons, R. L., Mangano, F., Macchi, A., & Piattelli, A. (2008). Direct laser metal sintering as a new approach to fabrication of an isoelastic functionally graded material for manufacture of porous titanium dental implants. *Dental Materials*, 24(11), 1525-1533.
- Utneja, S., Nawal, R. R., Talwar, S., & Verma, M. (2015). Current perspectives of bio-ceramic technology in endodontics: calcium enriched mixture cement - review of its composition, properties and applications. *Restorative Dentistry and Endodontics*, 40(1), 1-13.
- Wakily, H., Dabbagh, A., Abdullah, H., Halim, N. F. A., & Kasim, N. H. A. (2015). Improved thermal and mechanical properties in hydroxyapatite–titanium composites by incorporating silica-coated titanium. *Materials Letters*, 143, 322-325.
- Watanabe, Y., Kawamoto, A., & Matsuda, K. (2002). Particle size distributions in functionally graded materials fabricated by the centrifugal solid-particle method. *Composites Science and Technology*, 62(6), 881-888.

- Watari, F., Yokoyama, A., Omori, M., Hirai, T., Kondo, H., Uo, M., & Kawasaki, T. (2004). Biocompatibility of materials and development to functionally graded implant for bio-medical application. *Composites Science and Technology*, 64(6), 893-908.
- Watari, F., Yokoyama, A., Saso, F., Uo, M., & Kawasaki, T. (1997). Fabrication and properties of functionally graded dental implant. *Composites Part B: Engineering*, 28(1), 5-11.
- Weng, J., Liu, X., Zhang, X., & Ji, X. (1994). Thermal decomposition of hydroxyapatite structure induced by titanium and its dioxide. *Journal of Materials Science Letters*, 13(3), 159-161.
- Werner, A. J. (1969). Titanium dioxide pigment coated with silica and alumina: Google Patents.
- Wong, L. H., Tio, B., & Miao, X. (2002). Functionally graded tricalcium phosphate/fluoroapatite composites. *Materials Science and Engineering: C*, 20(1), 111-115.
- Xiao, X. F., Liu, R. F., & Zheng, Y. Z. (2005). Hydroxyapatite/titanium composite coating prepared by hydrothermal–electrochemical technique. *Materials Letters*, 59(13), 1660-1664.
- Yang, Y., Kim, K.-H., Agrawal, C. M., & Ong, J. L. (2004). Interaction of hydroxyapatite–titanium at elevated temperature in vacuum environment. *Biomaterials*, 25(15), 2927-2932.
- Ye, H., Liu, X., & Hong, H. (2009). Characterization of sintered titanium/hydroxyapatite biocomposite using FTIR spectroscopy. *Journal of Materials Science: Materials in Medicine*, 20(4), 843-850.
- Zhang, Y.-R., Du, W., Zhou, X.-D., & Yu, H.-Y. (2014). Review of research on the mechanical properties of the human tooth. *International Journal of Oral Science*, 6(2), 61-69.
- Zhou, C., Deng, C., Chen, X., Zhao, X., Chen, Y., Fan, Y., & Zhang, X. (2015). Mechanical and biological properties of the micro-/nano-grain functionally graded hydroxyapatite bioceramics for bone tissue engineering. *Journal of the Mechanical Behavior of Biomedical Materials*, 48, 1-11.